Sveriges lantbruksuniversitet
Swedish University of Agricultural Sciences

Faculty of Veterinary Medicine and Animal Science

Canine cone electroretinograms in response to visible and ultraviolet lights

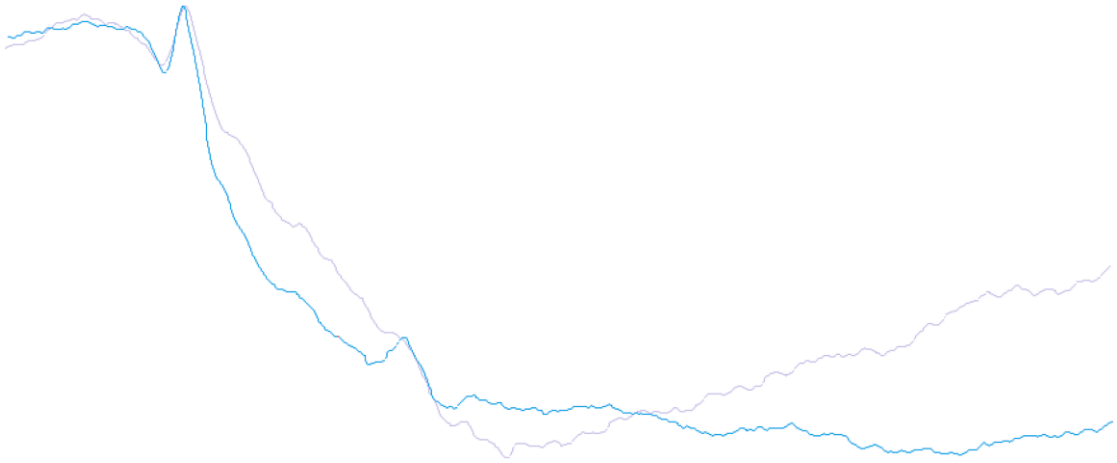

Lars Nordling

Uppsala
2019

Degree Project 30 credits within the Veterinary Medicine Programme

Canine cone electroretinograms in response to visible and ultraviolet lights

Lars Nordling

Supervisor: *Björn Ekesten, Department of Clinical Sciences*

Examiner: *Henrik Rönnberg, Department of Clinical Sciences*

Degree Project in Veterinary Medicine

Credits*: 30*
Level*: Second cycle, A2E*
Course code*: EX0869*

Place of publication*: Uppsala*
Year of publication*: 2019*
Online publication*: https://stud.epsilon.slu.se*
Cover illustration*: UV & S-cone ERG superimposed*

Key words*: dog, ERG, Electroretinography, M/L-cones, retina, S-cones, UV, Ultraviolet, vision*
Nyckelord*: ERG, Elektroretinografi, hund, M/L-tappar, näthinna, syn, S-tappar, UV, Ultraviolett*

Sveriges lantbruksuniversitet
Swedish University of Agricultural Sciences

Faculty of Veterinary Medicine and Animal Science
Department of Clinical Sciences

SUMMARY

Although ultraviolet (UV-) sensitivity has long been known to be widespread among invertebrates, birds and some rodents, recent studies have revealed that the ocular media of most mammals (unlike man) transmits a large amount of the UV-A wavelengths. In addition to rod cells, the domestic dog has two discrete types of cone photoreceptors. The peak sensitivity of the short wavelength-sensitive cones (S-cones) is in the blue to violet spectral range and the medium- to long-wavelength-sensitive cones have their peak sensitivity in the red to green part of the spectrum. In addition to the peak sensitive range (the α-band), the photosensitive cone pigment will to some degree also absorb photons of shorter wavelengths: β-band absorption. This extends the visible spectrum, theoretically reaching into the UV-part of the spectrum.

Full-field, flash electroretinography (fERG) is a non-invasive procedure that can be used to evaluate electrophysiological responses from the retinal cells. The fERG produces a two-dimensional waveform, which can be analyzed according to established guidelines. By stimulating the retina with wavelengths near the peak sensitivity of the S- or M/L-type cones along with continuous chromatic background illumination that desensitizes the responses from the rods and other type of cone (selective chromatic adaptation), it is possible to separate the responses from specific cell types.

This study details ERG exams performed on 9 healthy research dogs at the Swedish University of Agricultural Sciences to evaluate the UV-sensitivity of the canine cone photoreceptors. Using visible short- and long wavelengths, ERG recordings of S- and M/L- responses intended as a comparative baseline were obtained before also using UV-stimuli. Our results show that responses to different colored stimuli on a rod saturating and selective chromatic background can be used to obtain exclusive ML-cone driven responses and predominantly S-cone driven responses, respectively and indicate that both the S- and the M/L-cones are sensitive to stimuli in the UVA-range, although to different degrees.

CONTENTS

ABBREVIATIONS

ERG	electoretinogram
fERG	flash electroretinography
LED	light emitting diode
M/L-cones	medium to long wavelength cones
PRA	progressive retinal atrophy
RPE	retinal pigment epithelium
S-cones	short wavelength cones.
UV	ultraviolet wavelengths

INTRODUCTION

Due to the absorbance of our ocular media, ultraviolet (UV-) light is outside the chromatic range of man (Bowmaker & Dartnall, 1980; Anderson, 1983) and as a result, relatively little research has focused on the presence of ultraviolet vision in other mammals under the pretention that "if we don't, they don't". The earliest studies looking into UV photosensitivity were made by Sir John Lubbock, who published a series of papers throughout 1881 and 1883, describing experiments on ants (Lubbock, 1881, 1883). By taking advantage of the ants' natural instinct to hide their eggs when exposed he was able to show they could perceive UV-wavelengths. Since, UV-sensitivity has been discovered in a number of species: fish (Neumeyer, 1985), birds (Bowmaker, 1980), reptiles (Arnold & Neumeyer, 1987) and small mammals (Jacobs *et al*., 1991) among others.

In 2011, Hogg *et al*. published a study on UV-sensitivity in Arctic reindeer, the first of its kind in large eyed mammals detailing UV-transparent optical media as well as electrophysiological responses from the retina as a result of UV-stimulation (Hogg *et al*., 2011). A major comparative study in 2014 by Douglas and Jeffery revealed that most mammals, unlike man and other primates, absorb relatively little of UV-A spectrum wavelengths in their lenses (Douglas & Jeffery, 2014). The results from both studies are indicative that UV-sensitivity could be a more prominent vision enhancing mechanism in animals than previously presumed.

Advantages that come with UV-sensitivity in larger animals are presumably related to improved vision during low light periods by allowing more efficient use of available light e.g. during winter or for animals living on high altitudes (Hogg *et al*., 2011). The ancestral wolf (*Canis lupus*) likely had a crepuscular lifestyle, allowing them to hunt for prey during low light hours (Theuerkauf *et al*., 2003). Increased low light vision through UV-sensitivity thus makes sense and also goes in line with having developed a *tapetum lucidum*, which improves vision at the expense of visual acuity (Miller & Murphy, 1995). The study from Douglas and Jeffery (2014) details that the canine lens transmits up to 60% of UV-A spectrum wavelengths, but there is no evidence to support them having evolved mechanisms that reduce retinal damage due to UV exposure. High levels of UV-exposure during daytime has been shown to be a contributing factor for retinal disease in man (Chalam *et al*., 2011) and in becoming man's best friend, the domestic dog (*Canis familiaris*) has adopted a more diurnal lifestyle. It remains to be seen whether they have found an alternate way to avoid UV-related retinal damage or if it is of little consequence due to a comparatively short lifespan.

Visual sensitivity is the evolutionary product of the photic environment acting as a primary selective pressure. As such, there is a spread of chromatic vision among most vertebrates: nocturnal species that generally evolved a rod-dominated retina have sacrificed chromatic capacity in favor of improved low light vision (Jacobs *et al.*, 1993), whereas diurnal species evolved a more cone-rich retina with more than one cone class and a larger chromatic range (Bowman, 2008). Although chromatic sensitivity is relatively widely studied, it is indicative but not equal to chromatic range. Where the former is obviously a requirement for the latter, the latter is not necessarily a product of the former. Photosensitivity merely describes the capacity to respond to light of a specific wavelength, whereas chromatic vision entails pattern visualization as well as visual imaging and recognition of objects emitting or reflecting light of

different wavelengths. Sensitivity without vision could prompt stereotypical responses, e.g. as recognition of UV-light as harmful or dangerous resulting in avoidance (Menzel 1979; Kelber & Osorio 2010). As such, a wide range of photosensitivity lends to a larger chromatic capacity, however only behavioral studies can reveal if the entire chromatic range is used for image-forming vision and such studies are unfortunately few and far between (Kelber *et al*., 2003).

The aim of this study was to further research on canine ocular physiology in an attempt shed additional light on canine UV-photosensitivity and its responsible retinal cells, proving the hypothesis that the retina of the domestic dog is sensitive to UV light.

LITERARY REVIEW

Retinal structure

The retina is comprised of two principal layers (see figure 1 for schematic illustration). The outermost layer is the *retinal pigment epithet-lium* (RPE), a monolayer of cells that forms part of the outer blood-retinal barrier between the photoreceptor cells in the *neuroretina* and the choriocapillary blood supply. Its primary function is supportive: e.g. supplying nutrients and proteins required for photoreceptor regeneration / maintenance (including the chromophore) as well as removing cellular debris (Kiser *et al*., 2012; Strauss, 2012; Ofri, 2013). In addition, the cells in the RPE contain melanosomes: organelles with light-absorbing capabilities responsible for preventing photo-toxic damage to the retina by catching scattered light (Sarna, 1992).

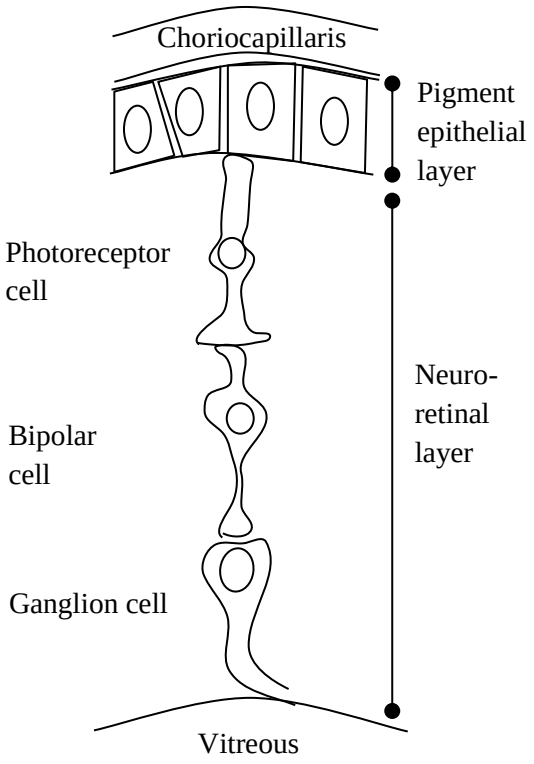

Figure 1. *Schematic overview of the retinal layers and its principal cells (Ofri, 2013).*

Closer to the center of the globe from the pigment epithelium is the neuroretina, housing the cells that convert photons to electrical impulses and propagate and modulate these responses (i.e. photoreceptor-, horizontal-, bipolar-, amacrine- and ganglion cells, as well as supportive glial elements) and eventually transmit these signals to the visual cortex of the brain where they are processed into vision (Ofri, 2013).

The neuroretinal cells

First order neurons

In the outermost part of the neuroretina are the photoreceptor cells, i.e. rods and cones that contain light-sensitive photopigments. The properties of each type of photoreceptor lends to variable functionality: rods are far more light-sensitive than cones (up to 200 times more), but

also less responsive (up to 4 times slower) and are mainly responsible for vision under scotopic (dim) light conditions. Under bright (photopic) light conditions, the rod cells will be saturated and unresponsive, making vision purely cone-driven (Ofri, 2013).

By number, rods are far more common in the canine retina compared to cones. The peripheral retina is mostly rod populated and depending on localization, rod-to-cone ratios range from 41:1 to 22:1. Similar to the *fovea centralis* in man, where the cone to rod ratio heavily favors the cones, canids have a more cone populated area located lateral to the optic disc: the *area centralis*, believed to increase visual acuity (Mowat *et al*., 2008). The area centralis is also believed to be involved in canine, foveal, degenerative disease, like that found in the fovea or macular area of man (Beltran *et al.,* 2014)

The photopigments in rods and cones have two functionally separate parts: an opsin and a chromophore. The opsin is a membrane-bound g-protein that defines the range of photo-sensitivity by determining which wavelengths a specific photopigment will absorb. The light-sensitive chromophore is a vitamin-A-derivative, *retinal*, that uses energy provided by the opsin absorbing photons to isomerize from *11-cis-retinal* to *11-trans-retinal*, indirectly resulting in ion-channel closure and hyperpolarization of the photoreceptor, as well as modulation of the release of a neurotransmitter (glutamate) from the synaptic terminal. Once the stimulus ceases, the chromophore will return to its original conformation and the cell will return to a depolarized state. This process continuously hyper- and repolarizes the photoreceptor as light hits the retina and photons are absorbed by the opsin (Masland 2012; Molday & Moritz, 2015; Lamb, 2016).

Second order neurons

In-between the photoreceptor cells and the ganglion cells are bipolar cells. They transfer the signal created by the hyperpolarizing photoreceptors to the ganglion cells. The bipolar cells synapsing to cones are anatomically different from those connecting to rods, but there are also two basic physiological types: ON- and OFF-bipolar cells, responding either to onset or cessation of light stimulus, respectively (although this is a greatly simplified classification, as there are 12 physiologically separate types of bipolars). The physiological difference in the bipolar pathway allows for contrast (Masland, 2012; Ofri, 2013).

Horizontal cells provide an inhibitory feedback mechanism to the rods and cones. The horizontal cells spread laterally among the photoreceptors and modulate their output according to the average illumination of the retinal surface in the surrounding region. The purpose of this is to keep the output within a limited range, making extremely bright objects appear dimmer while enhancing luminance (i.e. grayscale) and chromatic (i.e. color) contrast (Masland, 2012).

Amacrine cells form connecting networks between both the bipolar- and the ganglion cells. They are in involved in mechanisms distinguishing motion and directional movement, but also modulate bipolar cell output (i.e. ON-signals having an inhibitory effect on OFF- signals and vice versa) (Masland 2012; Vaney *et al*., 2012).

Third order neurons

At the opposing end of the neuroretina to the photoreceptor cells, closest to the vitreous body, are ganglion cells. On one end they synapse with the bipolar cells and on the other, their axons coalesce in the optic disc to form the optic nerve. They are the final stop before the visual signal departs the retina and makes its way toward the visual cortex of the brain for processing (Ofri, 2013).

Retinal glial cells

Müller cells are the most commonly found glial cells in the retinal population and like most glial cells, they perform supportive functions for the surrounding neurons. Among their principal duties, they supply nutrients, clear cell debris and recycle excess neurotransmitters and extracellular ions (Reichenbach & Robinson, 1995). Astrocytes are found enveloping the ganglion cell axons and retinal blood vessels and presumably constitute part of the blood-brain barrier (Schnitzer, 1988). The last types of glial cell found in the retina are microglia and oligodendrocytes. Microglia populate all layers of the retina, mainly responsible for phagocytosis of degenerated retinal cells (Boycott & Hopkins, 1981), whereas oligodendrocytes (found in some species, among other canines) act as insulating sheaths to axons throughout the central nervous system (Bradl & Lassmann, 2010).

Physiology of vision

Chromatic vision relies on having multiple cone opsins allowing for wavelength differentiation. All mammalian rod photoreceptor cells have the same photosensitive opsin; *rhodopsin*, with peak sensitivity at about 500 nm in most species. Genetically, there are four separate types of cone opsins in vertebrates, each one with a spectrally limited range. Middle- to long-wave class opsins (M/L-) have peak sensitivity at 490-570 nm in the red to green spectrum, whereas middle-wave class opsins (M-) peak at 480-535 nm in the green spectrum. Short-wave class type 2 (S2) are sensitive in the violet to blue spectrum, peaking at 410-490 nm and short-wave class type 1 (S1-) are sensitive in the ultraviolet to violet spectrum and peaks at 355-440 nm (Yokoyama, 2000; Bowmaker, 2008). The spectral sensitivity of similar opsins in different species is highly polymorphic due to genetic rearrangement (Jacobs *et al*., 1996).

Old World primates are trichromats, having three different types of cone opsins (M/L-, M- and S2-types). Most reptile- and avian species have all four types of vertebrate cone-opsins making them tetrachromats whereas most mammals, including the domestic dog, are dichromats with only two types of cone-opsins (M/L- and S2-types). The canine short-wavelength-sensitive cones (henceforth S-cones) have their peak sensitivity at 429 nm (blue) and medium- to long wavelength sensitive cones (henceforth M/L-cones) have peak sensitivity at 555 nm (green) (Neitz *et al*., 1989; Jacobs *et al*., 1993). The vast majority (roughly 90%) of the canine cone population are M/L-type (Mowat *et al*., 2008). Specific UV-sensitive cone opsins (S-1 type) are widespread among invertebrates, but are also found among some lower vertebrates (Hunt, 2001) and studies on rodents (Jacobs *et al*., 1991; Jacobs & Deegan 1994) and bats (Winter *et al*., 2003) have shown specific photoreceptor opsins (short-wave class type 1) with peak sensitivities in the UV-range.

Although characterized by their peak sensitivity, the spectral range of the cone opsins is not fully uniform. In addition to the α-band range (i.e. their peak sensitivity), opsins are, although to a lower degree, also sensitive to wavelengths in a shorter wavelength range, the β-band (Govardovskii *et al.*, 2000). Although the importance of the absorbance in this range is not fully understood, the result is a sensitivity overlap between different classes of opsins. In the case of the canine photoreceptors, the β-band sensitivity of the M/L-cone opsins overlaps with the peak of the S-cone opsins, while the S-cone opsins have β-band sensitivity that stretches into the ultraviolet spectrum (figure 2) (Jacobs, 1992). This means that wavelengths close to the peak sensitivity of the S-cone opsins are also absorbed by the M/L-cone opsins, although less efficiently. Furthermore, S- and possibly M/L-cone opsins are theoretically sensitive to UV-wavelengths, provided they reach the retina (Anderson, 1983).

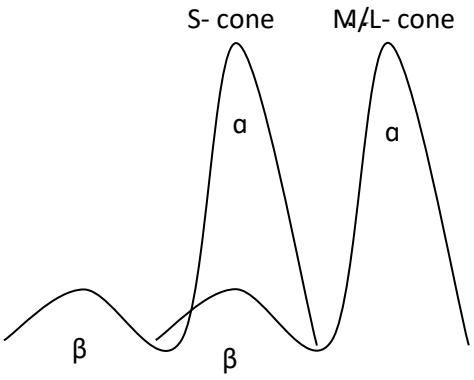

Figure 2. *Schematic representation of a- and β-band spectral sensitivity of the short-wave- and the medium to long-wave sensitive cones, loosely based on models by Govardovskii et al. (2000).*

Limitations of ultraviolet light & filtering by the ocular media

Due to the physiological limitations of the anatomy of the eye, UV-light sensitivity usually comes with a loss of visual acuity for most species due to chromatic aberration. Depending on the optical and anatomical characteristics of the eye, the focal point will vary according to the wavelength passing through the lens. As a result, only a specific wavelength will focus directly on the outer segments of the photoreceptors (where the light-sensitive photopigment resides), whereas all other wavelengths will be out of focus to some degree. Short wavelengths (e.g. UV) are more refracted than middle- and longer wavelengths and will be focused in front of the outer segments when, for example, a green wavelength is perfectly focused on the light-sensitive outer segment. Longer wavelengths (e.g. red) will similarly be out of focus, but instead focus behind the retina (figure 3) (Cronin & Bok, 2016).

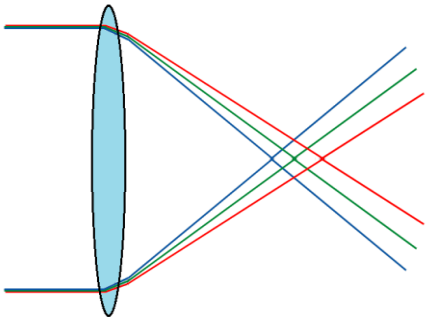

Figure 3. *Schematic representation of chromatic aberration reducing visual acuity. The focal point of different wavelengths will vary according to the properties of the optical media. As a result, certain wavelengths will result in a loss of visual acuity, making objects appear smaller or larger once they reach the photoreceptor cells (Cronin & Bok 2016).*

Chromatic aberration increases in a larger sized eye due to a larger curvature of the cornea (given that the properties of the ocular media are similar to that of a shorter globe) and as most vertebrates have large eyes, many have evolved mechanisms to filter light that causes loss of acuity. The spectral transmission of any structure is determined by its thickness, structural

components and/or absorbing pigments. Oil drops in the avian retina and macular pigment in man are examples of mechanisms that prevents light from reaching the retina. Whereas billfish completely block UV-wavelengths (Fritsches *et al*., 2000), some species have changed the curvature of the lens to reduce refraction (i.e. chromatic aberration) and several avian species have even evolved multifocal lenses, allowing for multiple focal points (Lind *et al*., 2014).

Electroretinography used to study the retinal cells

Electroretinography (ERG) is the most commonly used electrophysiological test of retinal function. The electric potential generated by the retinal cells when stimulated with flashes or patterns of light is measured between two electrodes placed on the cornea and the skin close to the eye. Full-field flash electroretinography (fERG) exposes the entire retina equally to a rapid flash of light and is the preferred procedure in veterinary ophthalmology, as it requires the least cooperation from the patient and is generally performed under general anesthesia or sedation (Ekesten *et al*., 2013). Using different stimulus and background light conditions, detailed assessment of different retinal cells and pathways is possible.

With brief flashes of light (e.g. 5 ms) the ON- and OFF-bipolar responses will superimpose on the ERG (due to the limits of time and the detail of the recording). Although rarely used in veterinary ophthalmology, a longer exposure time (e.g. 100 ms) allows temporal separation of the responses to onset and cessation of the stimulus (Zrenner & Gouras 1979; Evers & Gouras 1986).

Selective chromatic adaptation

Bright chromatic light has been suggested to suppress the responses of both rods and cones on the ERG by desensitizing the opsins. The light-sensitive rods are easily saturated by most bright lights in the visible part of the spectrum and by using a background light with wavelengths close to the peak spectral sensitivity of either type of cone, it is theoretically possible to suppress the responses of a particular cone population as an aid to separate the cone populations according spectral sensitivity. Adding a stimulus of a different wavelength close to the absorption maximum of the non-suppressed cones can then be used to produce a response from the unsaturated cones (Zrenner & Gouras 1979; Kremers *et al*., 2003).

ERG and retinal disease

Studies on retinal disease in man have shown S-type cones to be more prone to pathology, both in ocular disease, as well as in systemic disorders (Daley *et al*., 1987; Greenstein *et al*., 1989). Having no clinical protocol for separation of S- and ML-cone ERGs in dogs, little is known regarding cone-specific susceptibility in this species.

Progressive retinal atrophy (PRA) is a group of hereditary, progressive retinal diseases found in several breeds of the domestic dog (as well as cats). In the homologous *retinitis pigmentosa (RP)* in man, rod-cone dystrophy is classically characterized by night blindness and eventually loss of daylight vision and visual acuity, whereas a cone dystrophy often results in photophobia, loss of central vision, loss of color vision and impaired daylight vision in general. ERG can

potentially be used as a diagnostic tool to diagnose and differentiate between forms of PRA, as well as for providing early diagnosis before onset of other clinical signs (Turney *et al*., 2007).

Alzheimer's disease is an age-related neurodegenerative disease in man causing dementia without effective treatment. Alzheimer's has been shown to cause protein accumulation in the neuroretinal layer in animal models (Liu *et al*., 2009), resulting in retinal ganglion cell dysfunction that can be detected using ERG (Krasodomska *et al*., 2010). With advancements in healthcare, age-related diseases are becoming increasingly more common (Prince *et al*., 2015) and presumably a similar pattern will emerge with an aging population of domestic animals. Using ERG could turn out to be instrumental in early detection and diagnosis.

Hemeralopia, congenital day-blindness, is a cone-specific hereditary disease found among others in the Alaskan malamute breed. A common presentation is an ophthalmoscopically normal pup between eight and ten weeks old with poor vision primarily under photopic conditions. ERG shows the absence of cone responses and histopathology shows progressive cone degeneration (Aguirre & Rubin, 1975).

Components of the ERG

The ERG is a two-dimensional waveform and each cell-driven electrical response correlates to a deflection of the baseline potential. In the normal luminance- (flash-) driven ERG several separate events are discernable, each corresponding to the successive signal transmission. The part of the first negative deflection, the a-wave, is caused by the hyperpolarization of the photoreceptor cells. Immediately following this, the bipolar cells are depolarized with the ON- and OFF-bipolar cells corresponding with b- and d-waves respectively (Frishman, 2006). Both the b- and the d-wave are positive deflections, and the d-wave (caused by stimulus cessation) can be separated from the a-b complex using long stimulus duration. When using short duration stimuli, the d-wave will be superimposed on the b-wave and the two will be indiscernible from one another. The i-wave is a small, positive deflection sometimes seen after the b-wave in short duration photopic ERGs, believed to originate from the retinal ganglion cells (Rosolen *et al*., 2004). The c-wave is derived from the hyperpolarization of the retinal pigment epithelium and Müller cells and can only be recorded using special D.C.-equipment (and is therefore not included in this study) (Pepperberg *et al*., 1978). Figure 4 shows an illustration of the aforementioned ERG events evaluated in this study.

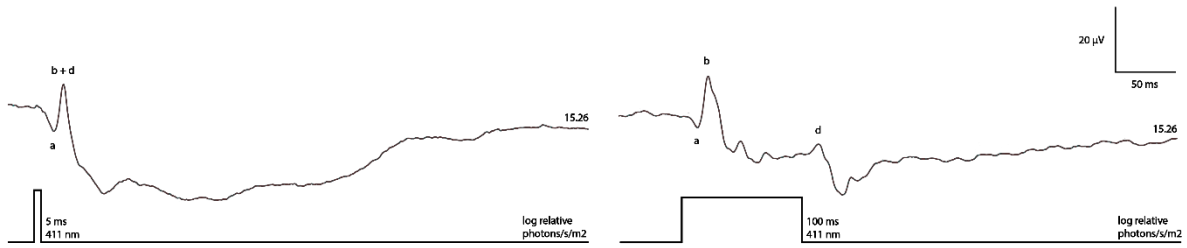

Figure 4. *Illustration of a canine ERG recording with 5 ms stimulus on the left and 100 ms on the right. Stimulus wavelength and duration is represented with a solid line beneath the ERG. Stimulus intensity is represented by log relative photons/s/m^2 on the end of each ERG curve.*

In addition to the overall waveform characteristics, two parameters are measured on the ERG waveform: the amplitude (i.e. the height of a response) and the time-to-peak or implicit time (i.e. the time from the onset of the stimulus to the peak of the response). The amplitude of each deflection corresponds to the strength of the retinal cell response or number of cells responding and is measured in microvolts. The implicit time corresponds to the speed of the cell response and is measured in milliseconds.

MATERIAL & METHODS

The data-set was collected from monocular ERG exams on 4 dogs in 2014 and 5 dogs in 2018. All animals were female research Beagles aged 1.5 to 6.5 years kept at the Department of Clinical Sciences, Swedish University of Agricultural Sciences, Uppsala, Sweden. A basic physical and ophthalmic examination prior to anesthesia was performed to assess the general health of the dog and absence of diseases potentially interfering with the study. All dogs were considered healthy at the time of the experiment without signs of dysfunction that would influence the results of the ERGs.

Ethical approval for the study was reviewed by the Uppsala Regional Ethical Review Board (C148/13).

Anesthetic protocol

Dogs were premedicated with intramuscular acepromazine (0.04-0.05 mg/kg, Plegicil vet., 10 mg/kg, Pharmaxin, Sweden) or dexmedetomidin (5 mg/kg, Cepedex, 0.5 mg/ml, VM Pharma, Germany) and anesthesia was induced with intravenous Propofol (6-8 mg/kg, PropVet Multidose, 10 mg/ml, Orion Pharma Animal Health, Finland). The dog was placed in ventral or lateral recumbency while anesthesia was maintained with continuous isoflurane (Attane vet, 1000 mg/g, Piramal Healthcare UK Ltd, Great Britain) and oxygene inhalation and monitored as per normal anesthetic protocol. All dogs were kept on preemptive continuous intravenous fluids throughout the anaesthesia (40 ml/kg/day Ringer-Acetate Baxter Viaflo, Baxter, Great Britain).

The ERG

Tropicamide and cyclopentolate eye drops (Cyclogyl, 1%, Mydriacyl, 0.5%, S.A. Alcon-Couvreur N.V., Belgium) were administered unilaterally for pupillary dilation prior to anesthetic induction. Dilation was evaluated before the experiment was initiated and conjunctival stay sutures in combination with a lid speculum kept the eyelids fully open throughout the exam.

A skin reference electrode (Gold Disc Electrodes, F-E5GH, Natus Neurology Inc., West Warwick, USA) was placed approximately 3 cm aborally of the lateral canthus of the eye after shaving and thorough cleaning using skin prepping gel (Nuprep Skin Prep Gel, D.O. Weaver & Co, Aurora, USA). A conductive paste (Ten20 Conductive, D.O. Weaver & Co, Aurora, USA) kept the electrode in position and enhanced conductivity. Using the same procedure, a ground electrode was placed at the vertex of the skull. Impedance between the two skin electrodes was kept well below 5 kOhms. A corneal contact lens electrode (JET-lens electrode, Universo, Switzerland) was used as the active electrode with artificial tears (Comfort Shield, 0.15%, i.com medical GmbH, Germany) as a coupling agent.

Light emitting diodes (LEDs; table 1) inside a custom-made mini-Ganzfeld stimulator (the inside of which was coated with white, spectrally flat, reflecting barium-sulphate paint) provided simultaneous background- and stimulus exposure. The LED output of the stimulus was incrementally adjusted along a rising intensity gradient by changing the voltage of a signal generator (Siglent SDG 5082, Ferner elektronik AB, Järfälla, Sweden), while the background remained the same throughout each exam. Following 10 minutes of adaptation to the chromatic background, either 5- or 100 ms flashes was presented at 0.5 Hz. Signals were amplified, digitally converted (PowerLab/8SP, AD Instruments Ltd., Dunedin, New Zealand) and saved using LabChart Pro software (AD Instruments Ltd., Dunedin, New Zealand). Sixteen to 30 responses were averaged for each ERG (for specific stimulus protocol, see table 2).

Table 1. *Specifications for the LEDs used for stimulus and background lights*

Color	Peak emittance	Manufacturer	Type
Red	627 nm	Philips Lumileds, San Jose, Ca., USA	Luxeon K2 red
Violet	411 nm	OSA Opto Light GmbH, Berlin, Germany	OCU-400 411 OS
Ultraviolet	365 nm	LED Engin, San Jose, Ca., USA	LZ1-00U600
Yellow	590 nm	Yoldal Co., LTD. Taipei, Taiwan	YSF-Y319EY

Table 2. *Stimulus and background protocols for the ERG exams*

Stimulus			Background			Intended response
Color	λ *(nm)*	Intensity *(log relative photons/s/m$^{2)}$*	Color	λ *(nm)*	Intensity *(log relative photons/s/m$^{2)}$*	
Red	627	12.7-14.9	Violet	411	14.3	M/L- response
Violet	411	10.8-14.3	Red	627	14.9	S- response
Ultraviolet	365	7.7-14	Red	627	14.9	UV M/L-response
Ultraviolet	365	7.7-14	Violet	411	14.3	UV S- response
Red	627	12,7-14.9	Yellow	590	14.4	M/L-desensitization

Calculation of stimulus intensity and data analysis

As per convention, the recorded data was plotted against the estimated amount of photons reaching the retina (corrected for ocular transparency (Douglas & Jeffery, 2014)), calculated with the Planck-Einstein relation:

$$E = h\,c \div \lambda$$

where E is the energy of a photon at λ wavelength, h is Planck's constant and c is the speed of light. Dividing E and the LED light output (measured in W/m^2 using a photometer (IL 1700, International Light Ltd, Newburyport, MA, USA)) at a specific voltage yields the relative number of photons per second per square meter.

All results were analyzed using JMP Statistical software (SAS Institute Inc., North Carolina, USA).

RESULTS

Cone desensitization

Figure 5 shows a response of long wavelength stimuli (ranging approximately 0.8 log units) on a long wavelength background. There are prominent a- and b-waves, where the b-wave amplitude increases with increasing stimulus intensity while the a-wave amplitude decreases (figure 6). The a- and b-wave wave implicit times become shorter throughout (figure 7). There is a sustained post b-wave hyperpolarization, but it plateaus just below the baseline. The plateau ends abruptly with a prominent d-wave on the brighter stimulus intensities.

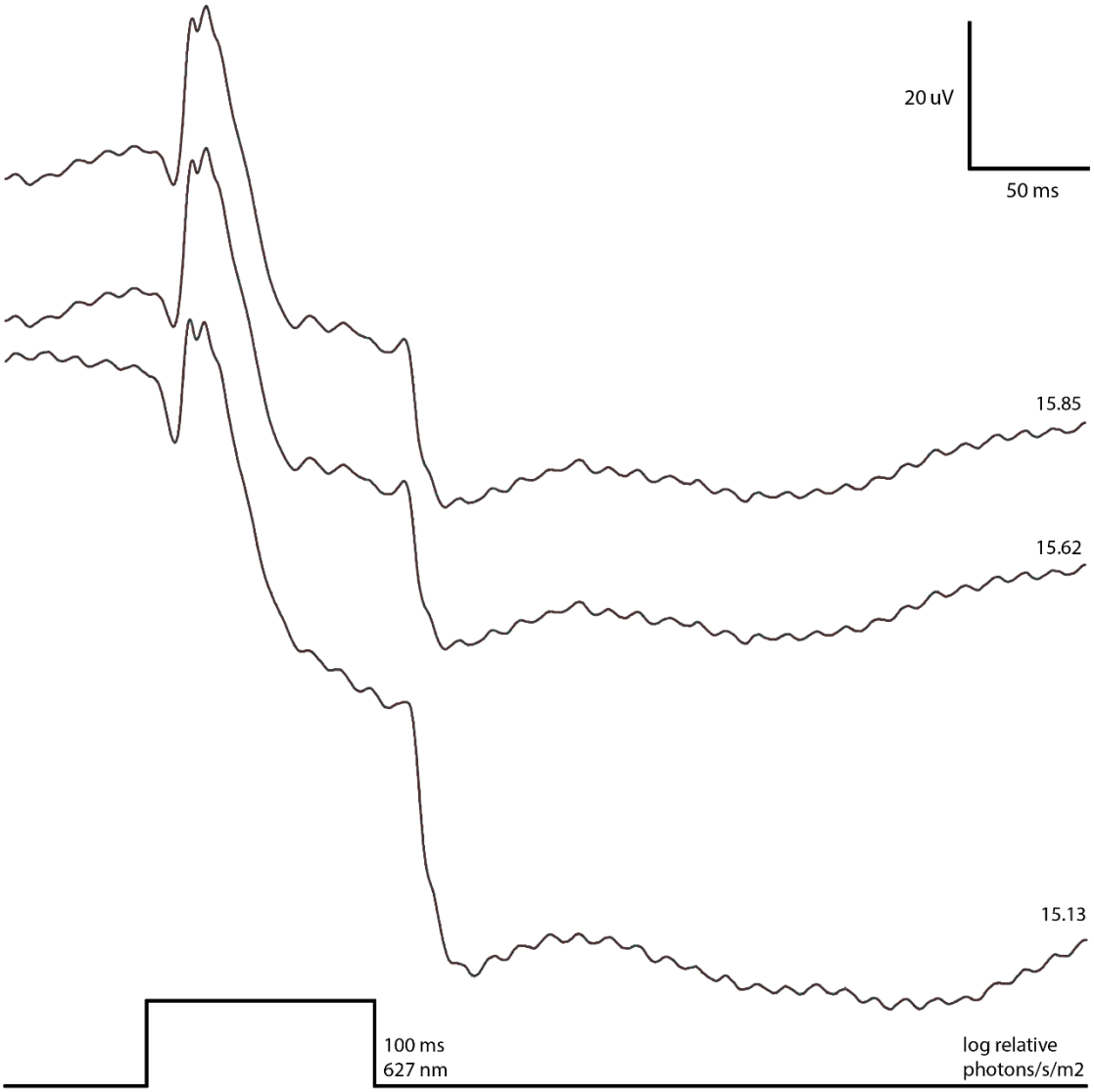

Figure 5. *ERG responses to 627 nm 100 ms stimulus on a 590 nm background (15.43 log relative photons/s/m^2). Stimulus wavelength and duration is represented with a solid line beneath the ERG. Stimulus intensity is represented by log relative photons/s/m^2 on the end of each ERG curve.*

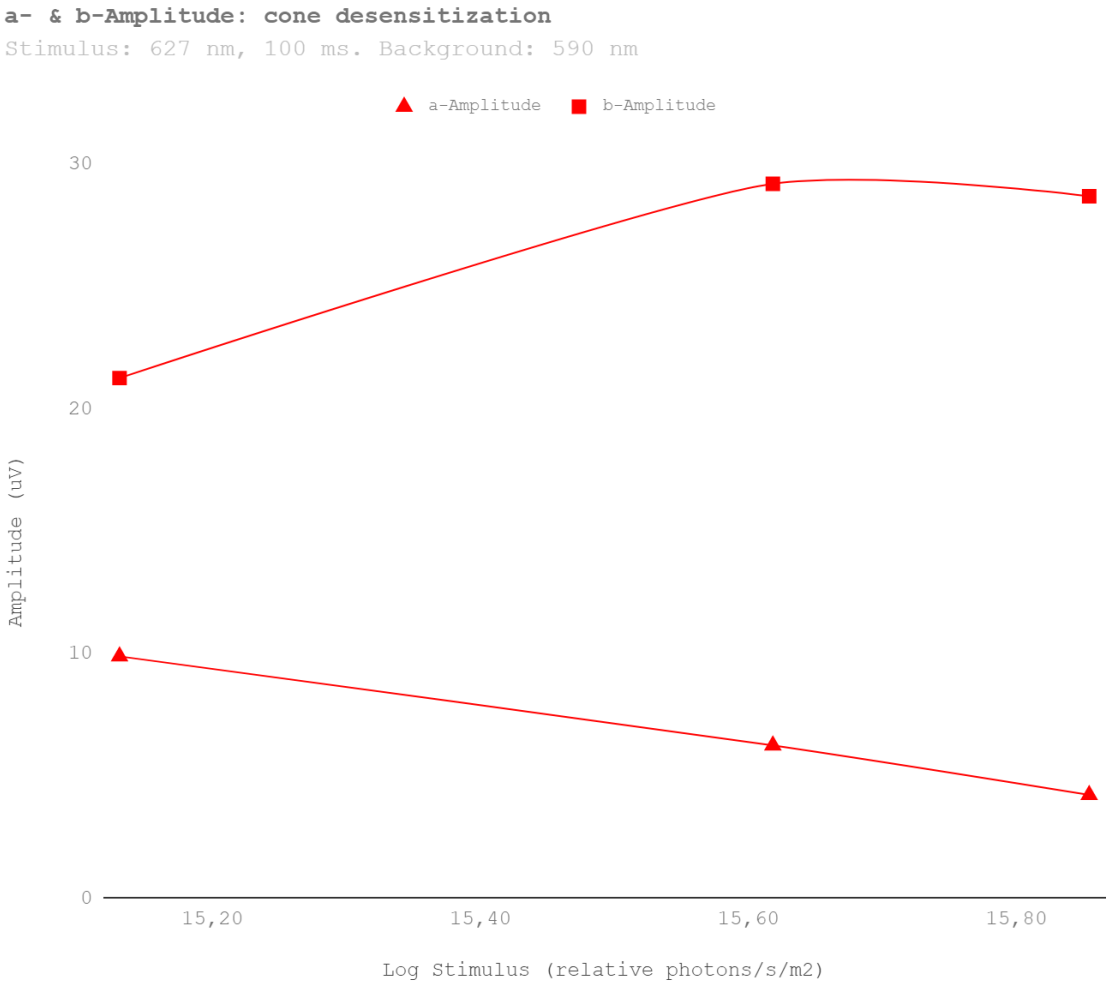

Figure 6. *Graph showing the a- and b-wave amplitude (μV) of 627 nm stimulus presented on a 590 nm background, plotted against stimulus intensity (relative photons/s/m^2).*

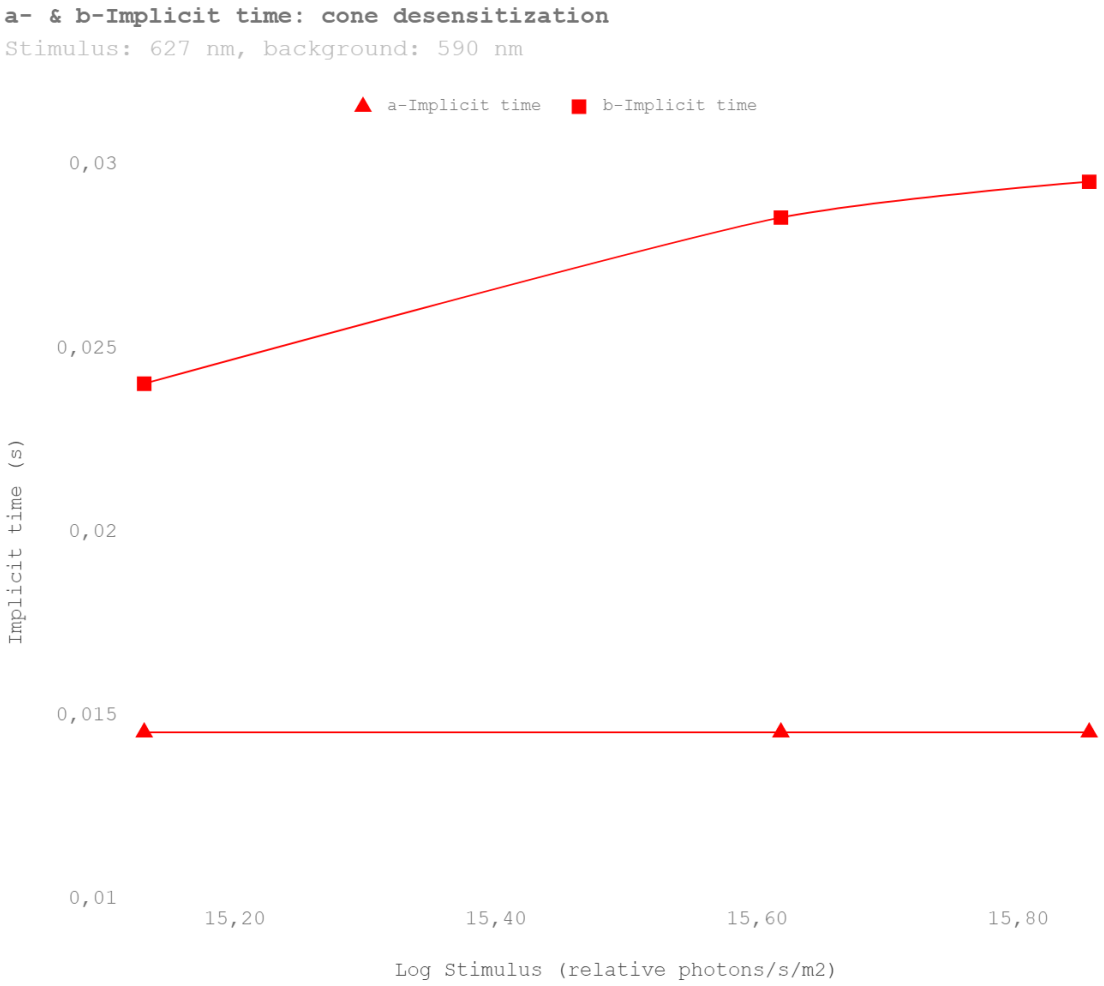

Figure 7. *Graph showing the implicit time (s) of 627 nm stimulus presented on a 590 nm background, plotted against stimulus intensity (relative photons/s/m^2).*

Red & violet stimulus

Figure 8 shows an ERG to short duration, short wavelength stimulus (violet) on a long wavelength (red) background and short duration, long wavelength stimulus (red) on a short wavelength (violet) background over an approximately 2 log-unit intensity range side by side. The waveforms of both ERGs show many similarities, with a prominent a-wave appearing before the b-wave and both a- and b-wave amplitudes increasing with increased stimulus intensity (figures 9 and 10). However, the responses were not univariant (the waveforms to the two different stimuli never become identical, no matter which stimulus intensities were used). The long wavelength stimulus ERG shows a prominent i-wave just after the b-wave.

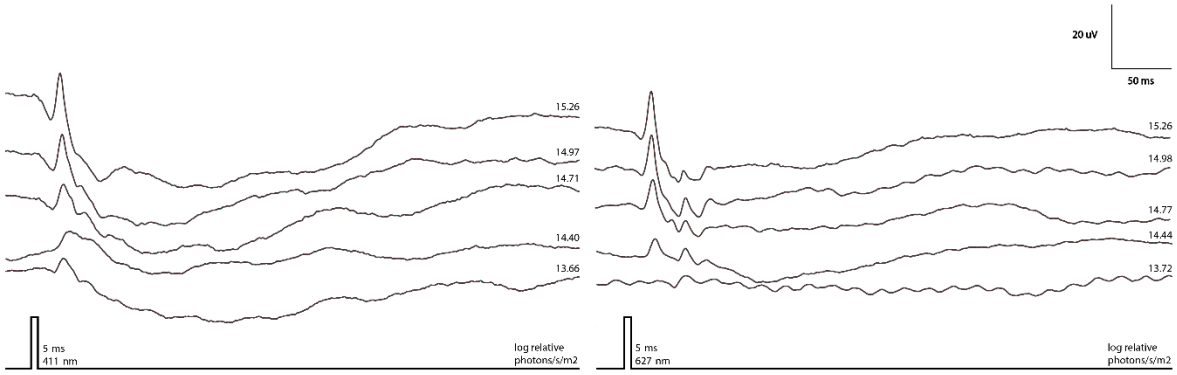

Figure 8. *ERG responses to 411 nm 5 ms stimulus on a log 627 nm background (15.26 log relative photons/s/m^2) to the left and 627 nm 5 ms stimulus on a log 411 nm background (log 15.26 photons/s/m^2) to the right. Stimulus wavelength and duration is represented with a solid line beneath the ERG. Stimulus intensity is represented by log relative photons/s/m^2 on the end of each ERG.*

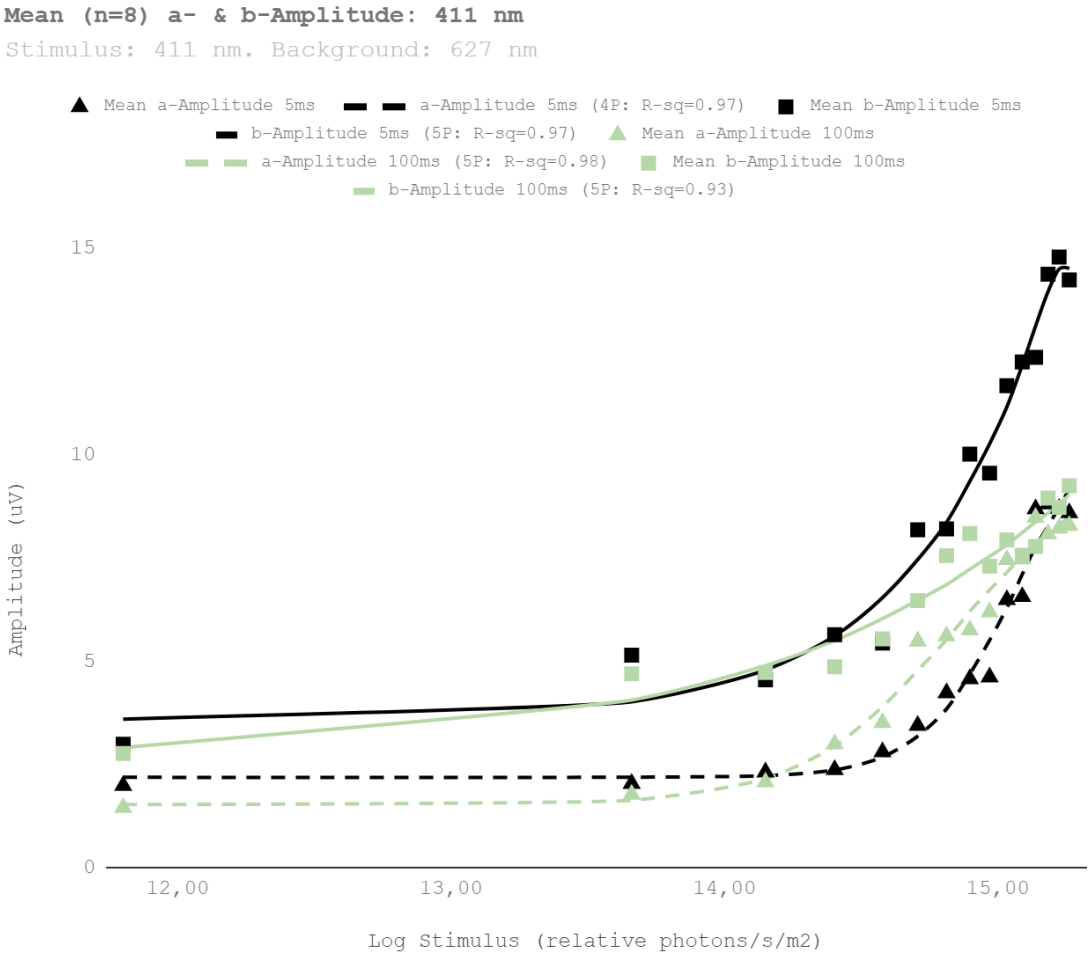

Figure 9. *Graph showing the a- and b-wave amplitude (μV) of 411 nm stimulus presented on a 627 nm background, plotted against stimulus intensity (relative photons/s/m^2). Data is presented along a 4- or 5-parameter logistic function.*

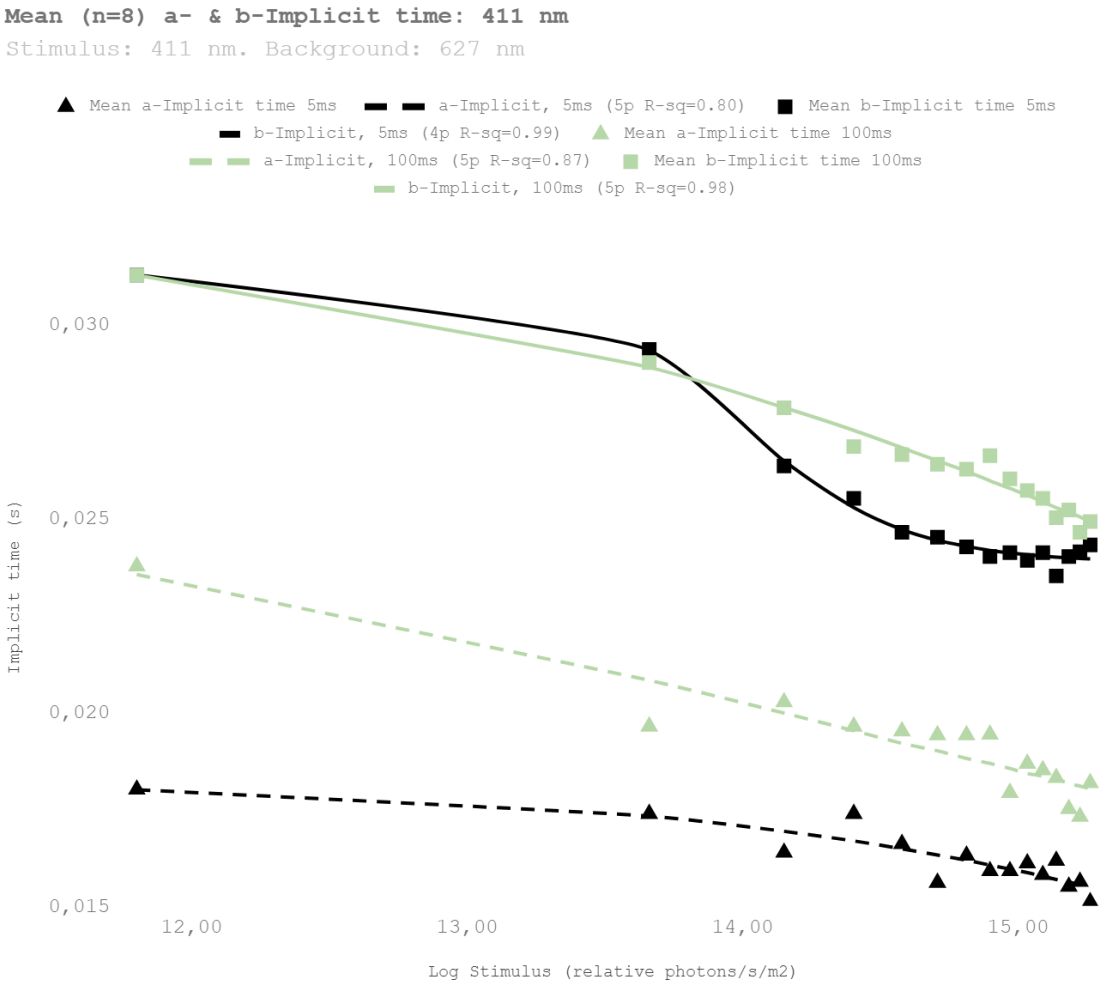

Figure 10. *Graph showing the a- and b-wave implicit time (s) of 411 nm stimulus presented on a 627 nm background, plotted against stimulus intensity (relative photons/s/m^2). Data is presented along a 4- or 5-parameter logistic function.*

Figure 11 shows ERGs to long duration, short wavelength stimuli on a long wavelength background and long duration, long wavelength stimuli on a short wavelength background over an approximately 2-log unit stimulus range side by side. The ERGs in response to the short wavelength stimuli had smaller a- and b-wave amplitudes compared to the long wavelength stimulus response. Implicit times were longer for the short wavelength stimulus than for responses to the long wavelength stimulus (figures 12 and 13) and the amplitudes of both the a- and b-waves increased in response to increased stimulus intensity while implicit time decreased with increasing stimulus intensities for both stimuli.

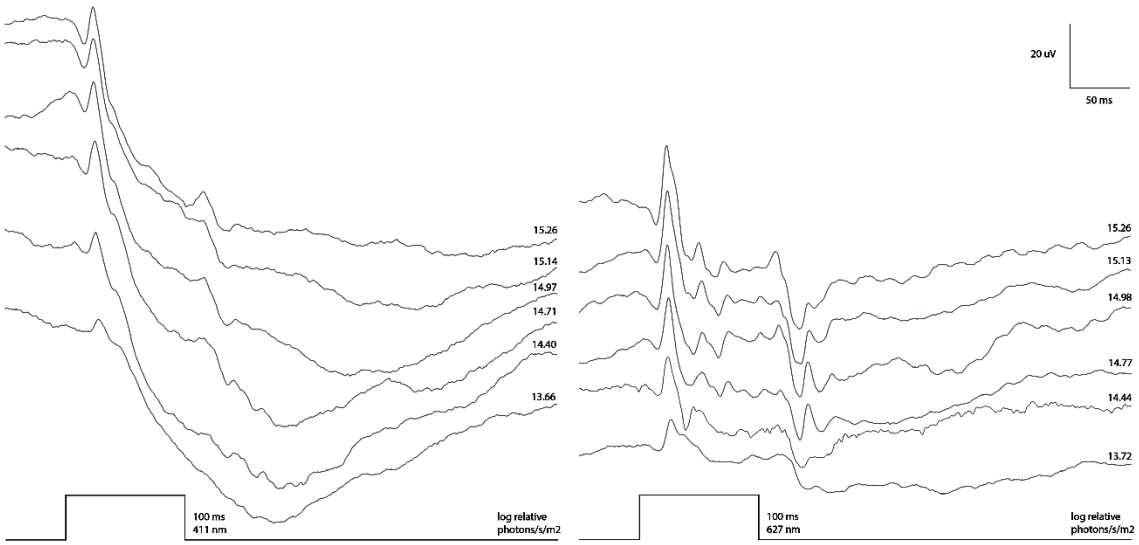

Figure 11. *ERG responses to 411 nm 100 ms stimulus on a 627 nm background (15.85 log relative photons/s/m^2) to the left and 627 nm 100 ms stimulus on a 411 nm background (15.26 log relative photons/s/m^2) to the right. Stimulus wavelength and duration is represented with a solid line beneath the ERG. Stimulus intensity is represented by log relative photons/s/m^2 on the end of each ERG.*

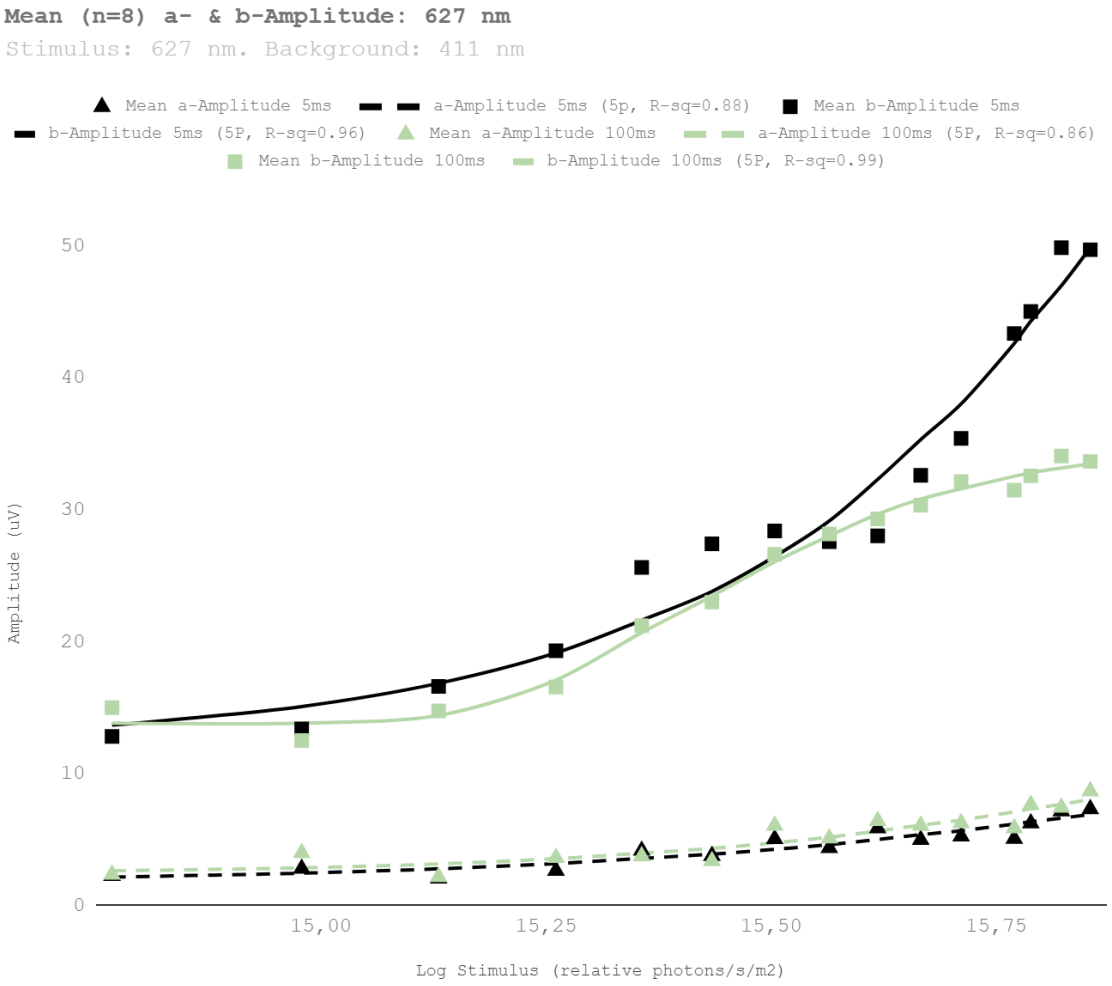

Figure 12. *Graph showing the a- and b-wave amplitude (μV) of 627 nm stimulus presented on a 411 nm background, plotted against stimulus intensity (relative photons/s/m^2). Data is presented along a 4- or 5- parameter logistic function.*

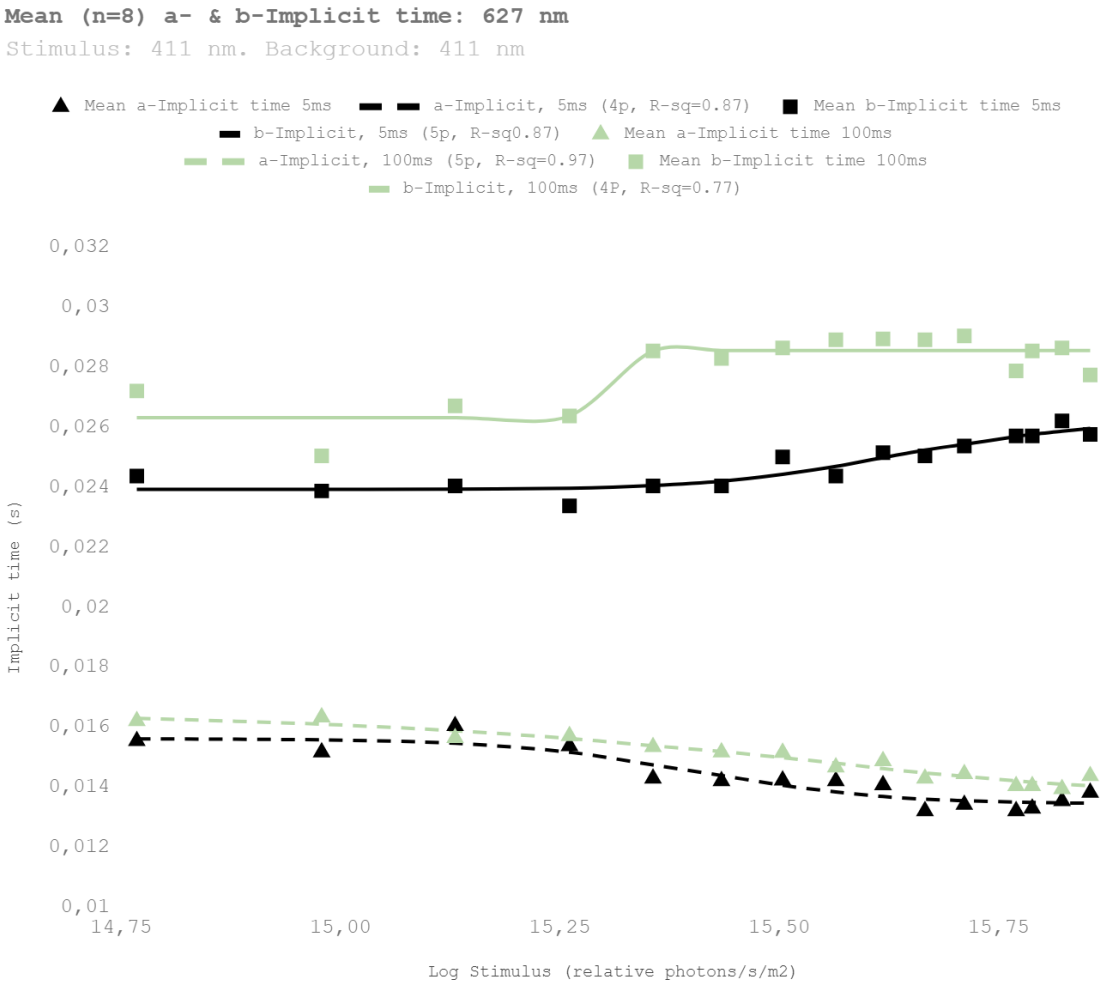

Figure 13. *Graph showing the a- and b-wave implicit time (ms) of 627 nm stimulus presented on a 411 nm background, plotted against stimulus intensity (relative photons/s/m^2). Data is presented along a 4- or 5-parameter logistic function.*

Figure 14 shows the ERG of 3 separate dogs to long duration, red stimuli at maximum intensity (15.85 log relative photons/s/m^2) on a bright violet background. The same overall characteristics that are seen in figure 11 are observed when the test is repeated in all dogs, although the amplitudes vary a bit. A d-wave can be observed in the tracings from all dogs, but is more prominent in two of them.

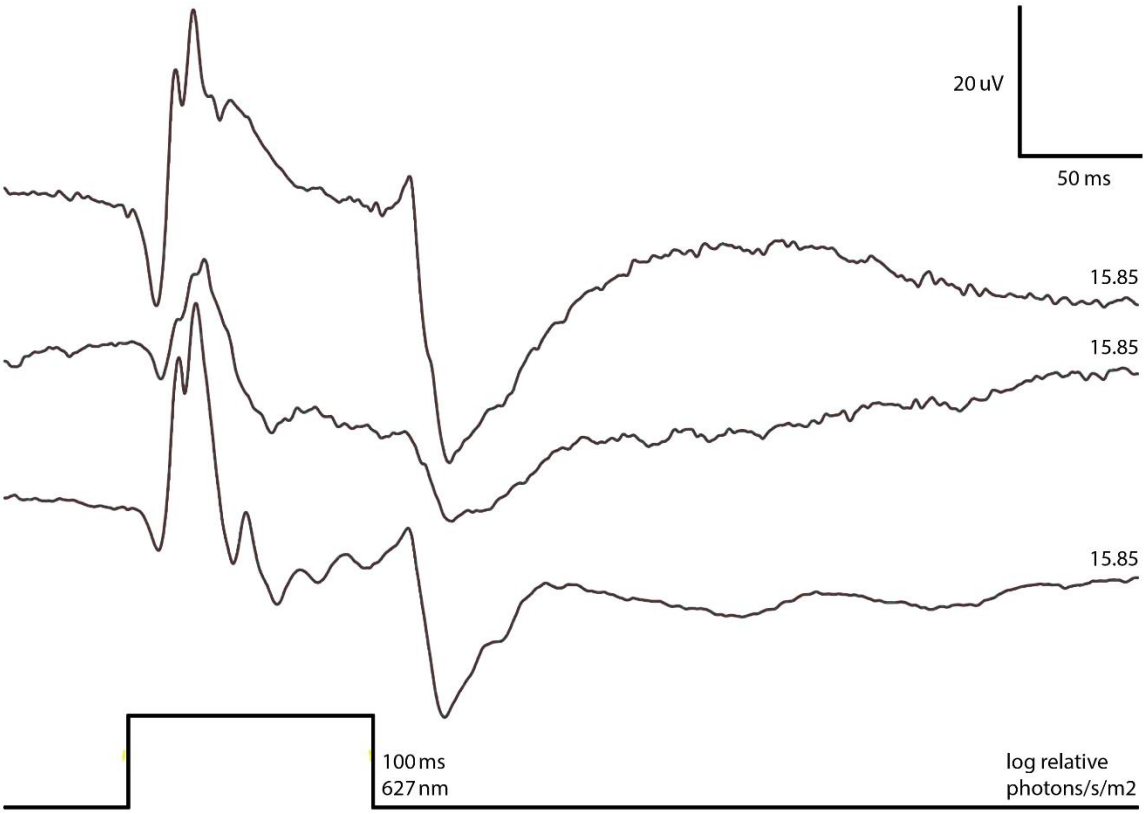

Figure 14. *ERG responses to 627 nm 100 ms stimulus on a 411 nm background (log 15.43 relative photons/s/m^2) in 3 dogs superimposed. Stimulus wavelength and duration is represented with a solid line beneath the ERG. Stimulus intensity for all ERG curves is 15.85 log relative photons/s/m^2.*

Figure 15 shows ERG responses of 3 separate dogs to long duration, violet stimulus at maximum intensity (15.26 log relative photons/s/m^2) on a bright red background. Similar overall characteristics that can be seen in figure 11 are also seen in the responses of all dogs, although the amplitudes vary with each response. A d-wave can be observed in the tracings from all dogs, but is more prominent in two of them. Figure 16 shows side by side comparisons of the violet 5 ms and 100 ms stimuli on the bright red background.

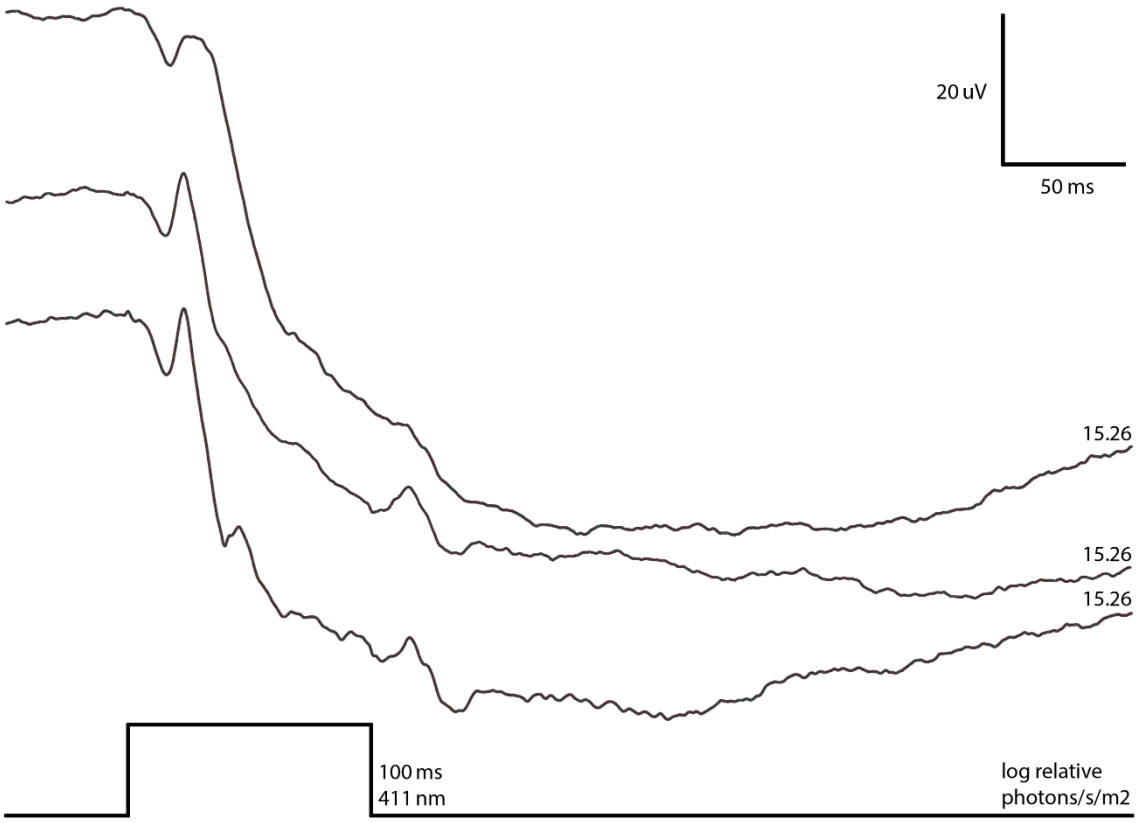

Figure 15. *ERG responses to 411 nm 100 ms stimulus on a 627 nm background (15.43 log relative photons/s/m^2) in 3 dogs compared Stimulus wavelength and duration is represented with a solid line beneath the ERG. Stimulus intensity for all ERG curves is 15.26 log relative photons/s/m^2.*

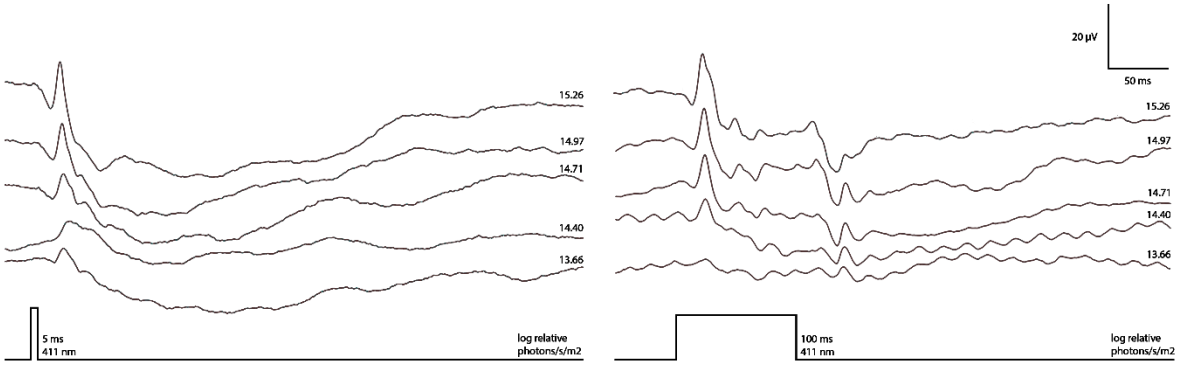

Figure 16. *Side by side comparison of ERGs to 627 nm 5 ms stimulus on a 627 nm background (15.26 log relative photons/s/m^2) to the left and 100 ms stimulus to the right. Stimulus wavelength and duration is represented with a solid line beneath the ERG. Stimulus intensity is represented by log relative photons/s/m^2 at the end of each ERG.*

Ultraviolet stimulus

Figure 17 shows ERGs throughout an approximately 1 log unit UV-wavelength intensity range on short and long wavelength backgrounds, respectively. Both the a- and b-wave amplitudes increase over the range of stimuli used, while the implicit time remains relatively stable (figures 18 and 19). The b-wave is followed by a prominent, sustained hyperpolarization before the response returns towards the baseline. Similarly, on the long wavelength background, the a-wave is not visible on the dimmest UV-flashes, although the b-wave is prominent. Both the a- and b-wave amplitude increase over the entire stimulus range. On the long stimulus background, the post b-wave hyperpolarization is less prominent and appears to plateau close to baseline. On the brighter stimulus intensities, the plateau ends with a prominent d-wave.

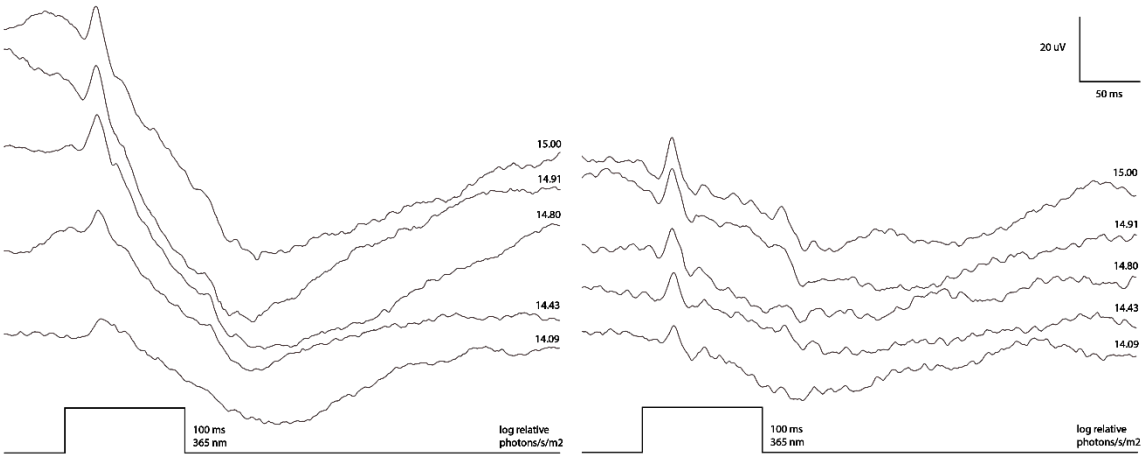

Figure 17. *ERGs to 365 nm 100 ms stimulus on a 590 nm background (15.43 log relative photons/s/m^2) to the left and 365 nm 100 ms stimulus on a 411 nm background (15.26 log relative photons/s/m^2) to the right. Stimulus wavelength and duration is represented with a solid line beneath the ERG.. Stimulus intensity is represented by log relative photons/s/m^2 on the end of each ERG.*

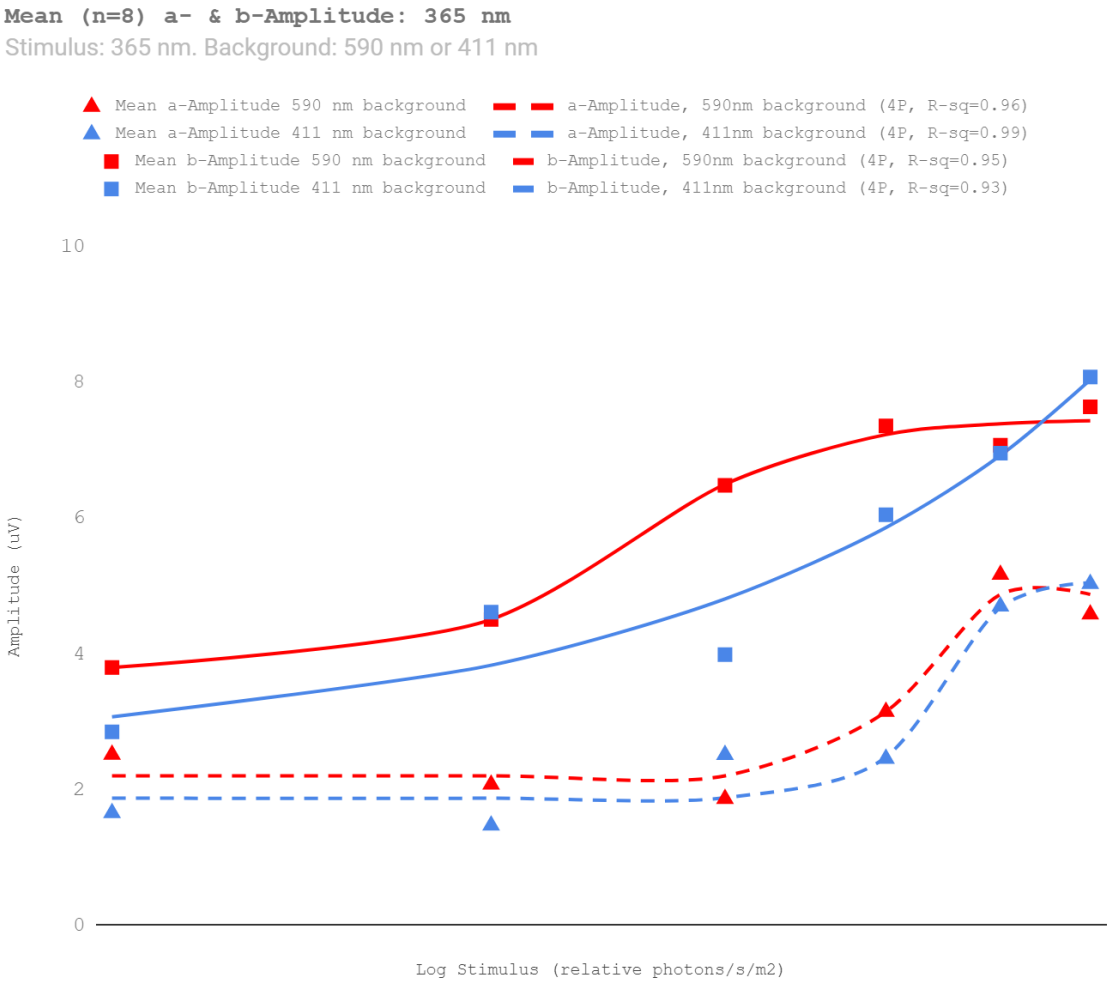

Figure 18. *Graph showing the a- and b-wave amplitude (μV) of 365 nm stimulus presented on a 590 nm or a 411 nm background, plotted against stimulus intensity (relative photons/s/m^2). Data is presented along a 4-parameter logistic function.*

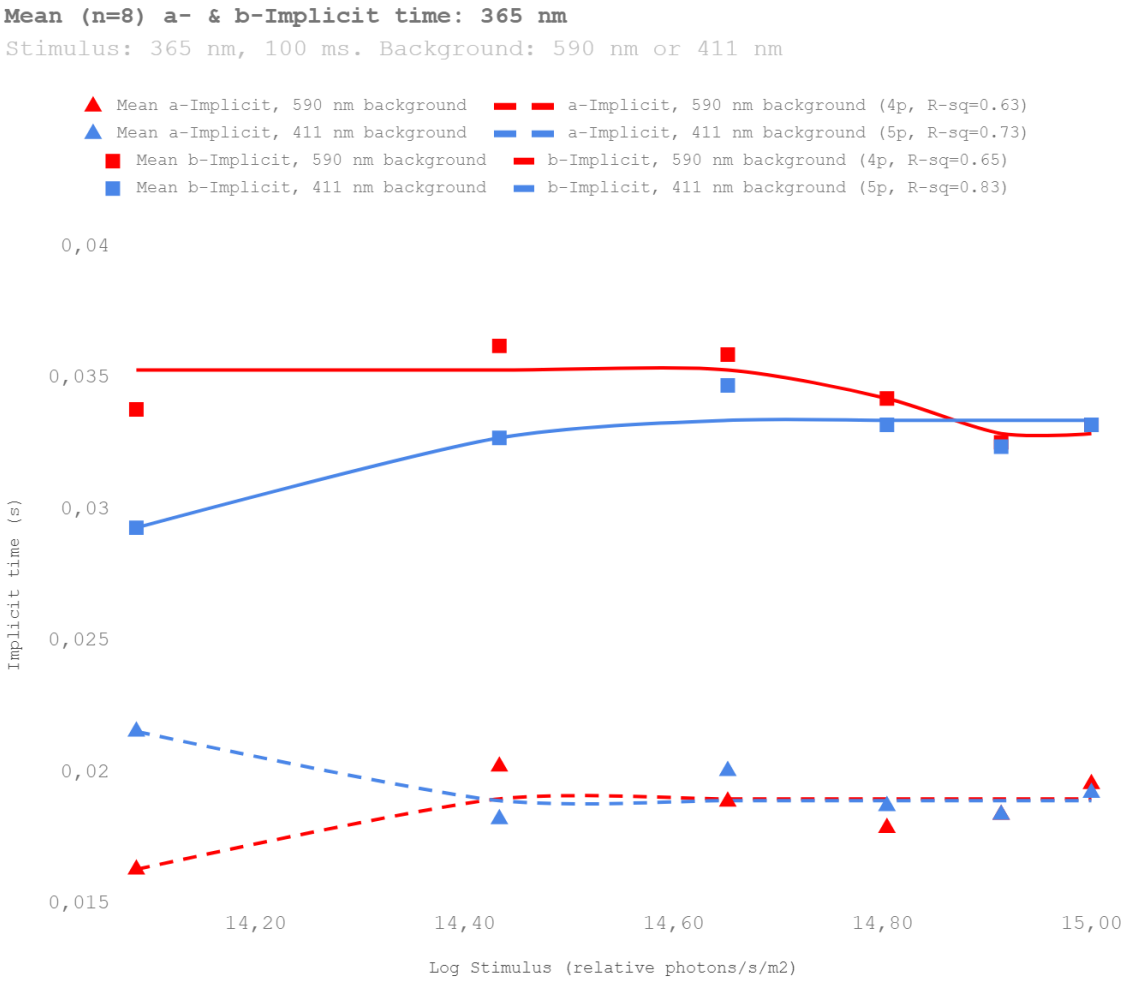

Figure 19. *Graph showing the a- and b-wave implicit times (ms) of 365 nm stimulus presented on 590 nm or 411 nm background, plotted against stimulus intensity (relative photons/s/m^2). Data is presented along a 4- or 5-parameter logistic function.*

Figures 20 and 21 show the ERG responses of 2 dogs to long duration, UV-wavelength stimulus on long and short wavelength backgrounds, respectively. The waveforms previously described for each stimulus protocol in figure 17 are very similar in all the dogs, although with varying amplitudes. On the long wavelength background, neither dog shows a prominent d-wave, whereas it can be seen in both on the short wavelength background.

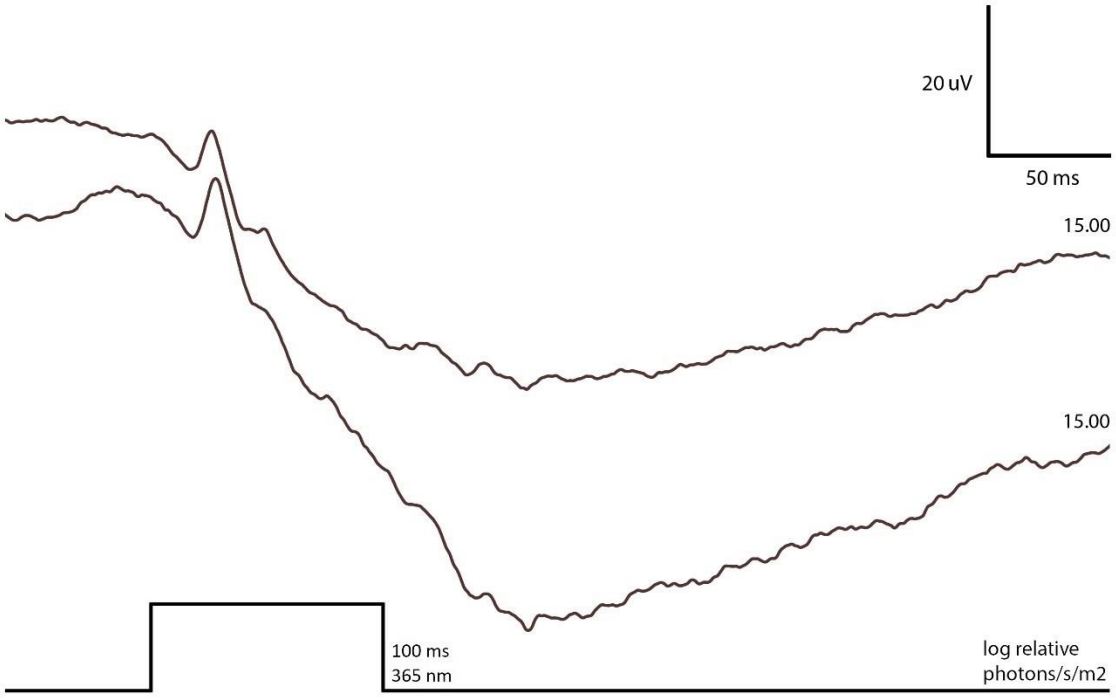

Figure 20. *ERGs to 365 nm 100 ms stimulus on a 590 nm background (15.43 log relative photons/s/m^2). Stimulus wavelength and duration is represented with a solid line beneath the ERG. Stimulus intensity is 15.00 log relative photons/s/m^2.*

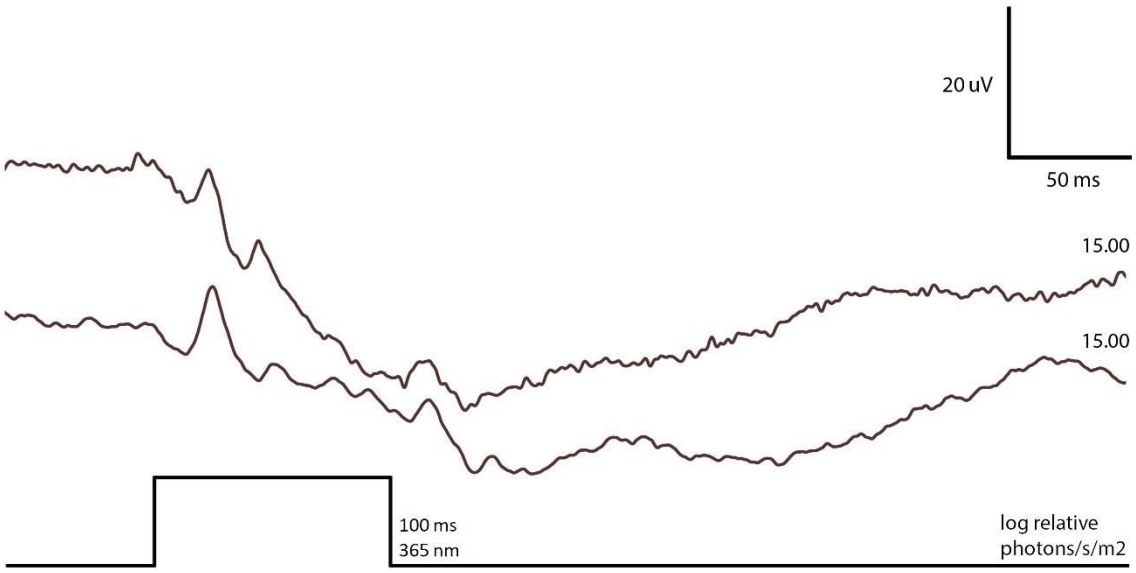

Figure 21. *ERGs to 365 nm 100 ms stimulus on a 411 nm background (15.26 log relative photons/s/m^2). Stimulus wavelength and duration is represented with a solid line beneath the ERG. Stimulus intensity is 15.00 log relative photons/s/m^2.*

DISCUSSION

Stimulus protocols

The LEDs for this study were chosen to match the peak wavelengths of either the S- or the M/L-cones reasonably well. The background light intensity was kept as bright as the signal generator would allow to saturate the rods and maximally desensitize the cone type not being stimulated by the flash stimulus (Zrenner & Gouras 1979; Kremers *et al*., 2003). Still, the short wavelength LED (411 nm) will not selectively stimulate the S-cones, due to the β-band absorption of the M/L-cones (Govardovskii *et al*., 2000). Although the M/L-β-band absorbance is likely to be small in relation to that of the S-cone α-band, the impact of the β-band absorption is difficult to evaluate because the M/L-cones outnumber the S-cones by far (Mowat *et al*., 2008; Beltran *et al.*, 2014). In order to isolate the S-cone response a long wavelength (627 nm) LED was used as a background, intended to desensitize the M/L-cones and saturate the rods.

As the S-cones are not sensitive to wavelengths above 520 nm, any response from a longer wavelength stimulus should theoretically be exclusively M/L-driven, which turned out to be key in comparing the response characteristics (Yokoyama, 2000; Bowmaker, 2008). The short wavelength LED used as a background to saturate the rod cells, inadvertently desensitized some of the M/L-cones through their β-band absorbance, however the effect of this was estimated to have little influence on the M/L-cone response, as this background would most likely only affect the ERG amplitudes and not the overall waveform (Govardovskii *et al*., 2000).

In order to test the efficacy of the M/L-cone saturation protocol, we used a long wavelength stimulus (627 nm) on a bright long wavelength background (590 nm). This stimulus would not be absorbed S-cones and the bright background was well above what is tolerated by the rods (Ofri, 2013). Unfortunately, the desensitization of the M/L-response was poor. The ideal would have been extremely small or even nonexistent response and instead it followed the same characteristics as the M/L-cone ERGs with similar, if not larger amplitudes to the same stimulus intensity. However, when comparing the amplitudes, the a-wave is smaller on the brightest stimulus, indicating at least some level of desensitization. We did not study the degree of S-cone desensitization on the short wavelength background, although it may not have been more effective than the long wavelength-background on the M/L-cones as the S-cones are unlikely to be affected by wavelengths we used for stimulating the M/L-cones (Yokoyama, 2000; Bowmaker, 2008). In addition, the S- to M/L-cone ratio makes it even less likely that any S-cones response would affect the M/L-type response (Mowat *et al*., 2008; Beltran *et al.* 2014). Either way, we cannot rule out that there is some degree of M/L-type contamination on the S-type responses, whereas the long-wavelength stimulus on the short-wavelength background must produce exclusive M/L-responses.

Long duration stimulus successfully separated ON- and OFF-bipolar responses with prominent d-waves commonly observed with 100 ms stimulus. Even considering some degree of M/L-cone contamination influencing the intended S-cone response, the waveforms of the 100 ms ERGs are obviously different from the exclusively M/L-driven response regardless of stimulus intensity, suggesting that there is a different pathway in play.

Ultraviolet wavelengths

We decided to focus on using the 100 ms responses for the UV-stimulations to obtain data regarding both the ON- and OFF-pathways. This was to increase the chances to figure out if light-adapted UV-responses were driven by the S- or M/L-cones or both cone classes by identifying similarities and differences compared to the putative S- and M/L-cone waveforms in our previous experiments. In addition, the risks associated with prolonged anesthesia were reduced.

The responses to UV-stimuli on short- and long-wavelength-backgrounds are markedly different, with the response of the intended M/L-desensitizing background having a more sustained post b-wave hyperpolarization compared to the ERGs obtained using the intended S-desensitizing background where the response has a more distinct plateau and prominent d-waves. The amplitudes are overall smaller than those seen in previous responses, but this is to be expected considering that the UV-stimulus hits the opsin outside the more sensitive α- band in both types of cones (Govardovskii *et al*., 2000). The characteristics of the intended M/L-desensitized UV-response is similar to that of the ERGs to short-wavelength stimuli (our putative S-driven ERG), while the intended S-desensitized UV-response displays similarities to the M/L-driven ERG. The amplitudes of the S-like UV-responses are larger compared to those of the M/L-like UV responses suggesting that S-cones are more efficiently absorbing light in in the UV-part of the spectrum, which makes sense in an evolutionary perspective, considering that the S-cones are closely related to the UV-sensitive pigments found in e.g. mice (Emerling *et al.*, 2015). However, the presence of an M/L-like response at all, indicates that the β-band range of the M/L cones reaches beyond the S-type spectrum into the ultraviolet. Taking the M/L- to S-cone ratios and the sizes of their responses into account, the M/L-cones seem to have a comparatively lower UV-sensitivity (Mowat *et al*., 2008; Beltran *et al.*, 2014).

Implications for canine vision

As previously mentioned, the ancestral history of the domestic dog suggests that there would be several advantages to UV-wavelength sensitivity, allowing for extended vision during periods of low light. Interestingly, our results suggest that both canine cone opsins absorb wavelengths in the UVA-part of the spectrum, but that they are not equally sensitive to the wavelength used in these experiments. Although speculative, this could imply that dogs are capable of differentiating between different wavelengths, "hues", within the very short-wavelength and UV-spectrum, theoretically allowing a form of color vision in this part of the spectrum. It is hard to theorize what the sensitivity means in terms of color without supporting behavioral studies, raising questions such as: are these relatively weak signals from the photoreceptors with possibly similar but not identical β-band absorption sufficient to drive color opponent ganglion cells?

Complicating factors that could influence the results

Besides the aforementioned risk of contamination from the suppressed cones, there are other potential factors that could have influenced the results. Age has been shown to influence the amplitude and implicit time of the b-wave in studies in man (Webler, 1981) as well as

correlating with accumulation of debris (lipofuscin) that could have influenced the results from the study (Moreno-Garciá *et al.*, 2018). Although the dogs in our study were relatively young, due to the limited sample population individual variation could be a factor. Even though there were no obvious signs of abnormal retinal appearance in the dogs used for this study, it is impossible to dismiss completely.

Improvements for successive studies

Ideally, the long wavelength LED would have had a smaller bandwidth and peak emittance closer to the absorption maximum of the M/L cone opsin (555nm) to maximize the effect on this cone class still without interfering with the S-cone opsin. Additionally, improving the desensitizing protocols to minimize contamination would enhance the interpretation of the results. To achieve this, I would recommend using a background light with higher efficacy. Most likely, our setup was simply too weak to allow for total desensitization. Alternatively, silent substitution could be used as an alternative to desensitization, allowing for less variables and potentially shorter anesthesia (Maguire *et al.*, 2016)

The output spectrum of the LEDs used varied, which would have made calculations of stimulus power more challenging if we wanted precise values. The red stimulus covered a much larger range, compared to that of the violet. Optimally, the range would be the same, making comparisons between stimuli easier.

Ideally, the study would also include a larger number of dogs, compensating for any natural variation in the ERG recordings.

CONCLUSION

We were able to isolate ERGs driven exclusively by M/L-cones in the canine retina. We have also isolated non-univariant waveforms predominantly driven by a strong stimulus for the S-cones on an M/L-desensitizing background, suggesting a strong input from the S-cones, even though we were unable to fully suppress the ML-cones with the background illumination.

We also show results indicating we were able to elicit responses from both type of cones through UV-stimulation of the retina. The M/L-type response to UV-light was considerably smaller compared to that of the putative S-type response, suggesting a lower sensitivity of the M/L-cones to UV-light, especially considering their numerical advantage. In summary, both cone-types seem to be sensitive to UV-wavelengths through their β-band absorbance.

ACKNOWLEDGEMENTS

I would like to thank my supervisor Björn Ekesten for endless patience and kindness, Fia Ryberg for expert technical assistance and Henrik Rönnberg for final proofreading. But most of all I would like to extend sincere gratitude to all unwilling participants without whom none of this would have been possible: Iris, Elsa, Maja, Zelda, Tuva, Nessie, Ginger, Belle and Saga.

POPULÄRVETENSKAPLIG SAMMANFATTNING

"Ljus" är egentligen en foton som rör sig i vågor och beroende på vågornas längd innehåller den olika mängd energi. Ultraviolett ljus ligger utanför det i dagligt tal "synliga" ljuset, då dess våglängd är mycket kort och i princip inte kan ses av människan. Det synliga ljuset innefattar allt ljus som vi, människor, kan uppfatta: rött, orange, gult, grönt, blått och lila.

För att vi ska se ljuset så tas det upp av specialiserade celler i näthinnan: tappar och stavar (fotoreceptorer). Stavarna är känsliga för små mängder ljus (enstaka fotoner) och svarar framförallt för mörkerseende, och de mindre känsliga tapparna ansvarar för färg- och dagsseende. Färgseende är en egenskap som beror på att det finns flera sorters tappar med olika ljuskänsliga pigment som vart och ett är känsligt för olika våglängder (färger). Detta innebär att hjärnan får signaler från och även kan jämföra signalerna från olika synceller med olika våglängdskänslighet och därigenom avgöra från vilken del av spektrat ljuset måste komma från och kan på så sätt skilja på olika färger.

Människan har tre olika sorters tappar vilket innebär att vi kan skilja på nyanser inom den kortvågiga (blå) till mellan- till långvågiga delen av spektrat (grönt till rött), men även skilja på nyanser som ligger mellan grönt och rött. De flesta däggdjur, däribland hundar, har bara två fotopigment och kan därmed bara se nyanser som ligger mellan den kortvågiga delen av spektrat och antingen de medellånga eller långa våglängderna. Det gör att de förmodligen har ett färgseende som röd- eller grönfärgblinda människor. Många ryggradslösa djur har fotopigment som är specialiserade för ultraviolett ljus (UV), men UV-känsliga pigment är relativt ovanligt hos ryggradsdjur (men förekommer hos exempelvis möss och råttor). Vidare finns det studier som visar att det blåa pigmentet till en viss grad också är känsligt för UV-ljus.

Då människans lins absorberar UV-ljus når mycket lite dessa våglängder näthinnan. I en studie från 2014 har forskare kunnat visa att till skillnad från människan så har de flesta andra däggdjur faktiskt en relativt hög genomsläpplighet av UV-ljus in till näthinnan. Av detta kan man då dra slutsatsen att människan haft evolutionär fördel av att minska genomsläppligheten för UV-ljus i ögat, men de flesta andra däggdjur istället haft en fördel av det. Nackdelarna med UV-ljuset är bland annat att det är skadligt; flera studier på människa har visat på ökad risk för näthinneskador associerade till UV-ljus. Därtill så minskar det skärpeseendet: allt ljus som kommer in i ögat kommer brytas, *fokuseras*, och beroende på våglängd så kommer ljuset att vara perfekt fokuserat framför, precis på eller bakom näthinnan. Grönt ljus blir väldigt bra fokuserat på näthinnan och ger bra skärpa, men de korta våglängderna fokuseras framför näthinnan, vilket gör att de kortare våglängderna (däribland blått och ultraviolett) träffar synceller vid sidan av dem som de skulle ha träffat om detta ljus var perfekt fokuserat och försämrar därför detaljupplösningen och gör bilden suddig. Fördelarna med UV-känslighet är med stor sannolikhet att det går att ta tillvara på större delar av det ljuset från himlen och på så sätt få ett bättre seende när solen står nära horisonten.

Funktionen hos ögats celler går att utvärdera med en metod som heter elektroretinografi (ERG). Med en ERG-undersökning kan man mäta det elektriska svaret som uppstår i ögat vid stimulering med olika våglängder av ljus. Genom att analysera skillnaderna som uppstår kan

man då isolera svaret från specifika celler. I den här studien gjordes ERG-undersökningar på totalt 9 hundar, varav 3 stimulerades med UV-ljus. Resultatet av undersökningarna antyder att båda typer av tappar i hundarnas näthinna har en känslighet för UV-ljus, men att den blå tappen är känsligare. Tyvärr så är det svårt att dra några konkreta slutsatser om hur detta påverkar hundens färgseende utan att också göra beteendestudier, men det förklarar varför vilda hunddjur ofta är grynings- och skymningsaktiva.

REFERENCES

Aguirre, G. & F Rubin, L. (1974). Pathology of hemeralopia in the Alaskan Malamute dog. *Investigative Ophthalmology*, 13, pp 231–5.

Anderson, R. M. (1983). Visual perceptions and observations of an aphakic surgeon. *Perceptual and Motor Skills*, 57(3 Pt 2), pp 1211–1218.

Arnold, K. & Neumeyer, C. (1987). Wavelength discrimination in the turtle Pseudemys scripta elegans. *Vision Research*, 27(9), pp 1501–1511.

Beltran, W.A., Cideciyan, A.V., Guziewicz, K.E., Iwabe, S., Swider, M., Scott, E.M., Savina, S.V., Ruthel, G., Stefano, F., Zhang, L., Zorger, R., Sumaroka, A., Jacobson, S.G. & Aguirre, G.D. (2014). Canine retina has a primate fovea-like bouquet of cone photoreceptors which is affected by inherited macular degenerations. *PloS One*, vol. 9 (3), pp. e90390–e90390.

Bowmaker, J. K. (1980). Birds see ultraviolet light. *Nature*, 284(5754), p 306.

Bowmaker, J. K. (2008). Evolution of vertebrate visual pigments. *Vision Research*, 48(20), pp 2022–2041 (Vision Research Reviews).

Bowmaker, J. K. & Dartnall, H. J. (1980). Visual pigments of rods and cones in a human retina. *Journal of Physiology*, 298, pp 501–511.

Boycott, B. B. & Hopkins, J. M. (1981). Microglia in the retina of monkey and other mammals; Its distinction from other types of glia and horizontal cells. *Neuroscience*, 6(4), pp 679–688.

Bradl, M. & Lassmann, H. (2010). Oligodendrocytes: biology and pathology. *Acta Neuropathologica*, vol. 119 (1), pp. 37–53.

Chalam, K. V., Khetpal, V., Rusovici, R. & Balaiya, S. (2011). A review: role of ultraviolet radiation in age-related macular degeneration. *Eye & Contact Lens*, 37(4), pp 225–232.

Cronin, T. W. & Bok, M. J. (2016). Photoreception and vision in the ultraviolet. *Journal of Experimental Biology*, 219(18), p 2790.

Daley, M. L., Watzke, R. C. & Riddle, M. C. (1987). Early loss of blue-sensitive color vision in patients with type I diabetes. *Diabetes Care*, 10(6), p 777.

Douglas, R. & Jeffery, G. (2014). The spectral transmission of ocular media suggests ultraviolet sensitivity is widespread among mammals. *Proceedings. Biological sciences / The Royal Society*, 281, p 20132995.

Miller, P. E., & Murphy, C. J. (1995). Vision in dogs. *Journal of the American Veterinary Medical Association*, 207, pp 1623-1634.

Ekesten, B., Komáromy, A. M., Ofri, R., Petersen-Jones, S. M. & Narfström, K. (2013). Guidelines for clinical electroretinography in the dog: 2012 update. *Documenta Ophthalmologica*, 127(2), pp 79–87.

Emerling, C.A., Huynh, H.T., Nguyen, M.A., Meredith, R.W. & Springer, M.S. (2015). Spectral shifts of mammalian ultraviolet-sensitive pigments (short wavelength-sensitive opsin 1) are associated with eye length and photic niche evolution. *Proceedings of the Royal Society B: Biological Sciences*, vol. 282 (1819), p. 20151817.

Evers, H. U. & Gouras, P. (1986). Three cone mechanisms in the primate electroretinogram: Two with, one without off-center bipolar responses. *Vision Research*, 26(2), pp 245–254.

Fritsches, K. A., Partridge, J. C., Pettigrew, J. D. & Marshall, N. J. (2000). Colour vision in billfish. *Philosophical Transactions of the Royal Society of London. Series B, Biological Sciences*, 355(1401), pp 1253–1256.

Goldsmith, T. H. (1980). Hummingbirds see near ultraviolet light. *Science (New York, N.Y.)*, 207(4432), pp 786–788.

Govardovskii, V. I., Fyhrquist, N., Reuter, T., Kuzmin, D. G. & Donner, K. (2000). In search of the visual pigment template. *Visual Neuroscience*, 17(4), pp 509–528.

Greenstein, V. C., Hood, D. C., Ritch, R., Steinberger, D. & Carr, R. E. (1989). S (blue) cone pathway vulnerability in retinitis pigmentosa, diabetes and glaucoma. *Investigative Ophthalmology & Visual Science*, 30(8), pp 1732–1737.

Hogg, C., Neveu, M., Stokkan, K.-A., Folkow, L., Cottrill, P., Douglas, R., Hunt, D. M. & Jeffery, G. (2011). Arctic reindeer extend their visual range into the ultraviolet. *Journal of Experimental Biology*, 214(12), pp 2014–2019.

Hunt, D. M., Wilkie, S. E., Bowmaker, J. K. & Poopalasundaram, S. (2001). Vision in the ultraviolet. *Cellular and Molecular Life Sciences CMLS*, 58(11), pp 1583–1598.

Jacobs, G. H. (1992). Ultraviolet vision in vertebrates. *American Zoologist*, 32(4), pp 544–554.

Jacobs, G.H., Deegan, J.F., Neitz, J., Crognale, M.A. & Neitz, M. (1993). Photopigments and color vision in the nocturnal monkey, Aotus. *Vision Research*, vol. 33 (13), pp. 1773–1783.

Jacobs, G. H. & Deegan, J. F. (1994). Sensitivity to ultraviolet light in the gerbil (Meriones unguiculatus): Characteristics and mechanisms. *Vision Research*, 34(11), pp 1433–1441 (The Biology of Ultraviolet Reception).

Jacobs, G. H., Deegan, J. F., Crognale, M. A. & Fenwick, J. A. (1993). Photopigments of dogs and foxes and their implications for canid vision. *Visual Neuroscience*, 10(1), pp 173–180.

Jacobs, G. H., Neitz, J. & Deegan Ii, J. F. (1991). Retinal receptors in rodents maximally sensitive to ultraviolet light. *Nature*, 353(6345), pp 655–656.

Jacobs, G. H., Neitz, M., Deegan, J. F. & Neitz, J. (1996). Trichromatic colour vision in New World monkeys. *Nature*, 382(6587), pp 156–158.

Kelber, A., Vorobyev, M. & Osorio, D. (2003). Animal colour vision - behavioural tests and physiological concepts. *Biological Reviews*, 78(1), pp 81–118.

Kelber, A. & Osorio, D. (2010). From spectral information to animal colour vision: experiments and concepts. *Proceedings of the Royal Society B: Biological Sciences*, 277(1688), pp 1617–1625.

Kiser, P. D., Golczak, M., Maeda, A. & Palczewski, K. (2012). Key enzymes of the retinoid (visual) cycle in vertebrate retina. *Biochimica et Biophysica Acta (BBA) - Molecular and Cell Biology of Lipids*, 1821(1), pp 137–151 (Retinoid and Lipid Metabolism).

Krasodomska, K., Lubiński, W., Potemkowski, A. & Honczarenko, K. (2010). Pattern electroretinogram (PERG) and pattern visual evoked potential (PVEP) in the early stages of Alzheimer's disease. *Documenta Ophthalmologica. Advances in Ophthalmology*, 121(2), pp 111–121.

Kremers, J., Stepien, M. W., Scholl, H. P. N. & Saito, C. (2003). Cone selective adaptation influences L- and M-cone driven signals in electroretinography and psychophysics. *Journal of Vision*, 3(2), pp 3–3.

Lamb, T. D. (2016). Why rods and cones? *Eye (London, England)*, 30(2), pp 179–185.

Liu, B., Rasool, S., Yang, Z., Glabe, C. G., Schreiber, S. S., Ge, J. & Tan, Z. (2009). Amyloid-peptide vaccinations reduce β-amyloid plaques but exacerbate vascular deposition and inflammation in the retina of Alzheimer's transgenic mice. *The American Journal of Pathology*, 175(5), pp 2099–2110.

Lubbock, J. (1881). Observations on ants, bees, and wasps.—Part VIII. *Zoological Journal of the Linnean Society*, 15(87), pp 362–387.

Lubbock, J. (1883). On the sense of color among some of the lower animals.—Part II. *Zoological Journal of the Linnean Society*, 17(100), pp 205–214.

Maguire, J., Parry, N.R.A., Kremers, J., Kommanapalli, D., Murray, I.J. & McKeefry, D.J. (2016). Rod electroretinograms elicited by silent substitution stimuli from the light-adapted human eye. *Translational Vision Science & Technology*, vol. 5 (4), pp. 13–13.

Masland, R. H. (2012). The neuronal organization of the retina. *Neuron*, 76(2), pp 266–280.

Menzel R. (1979). Spectral sensitivity and color vision in invertebrates. In: Autrum H. (ed.) *Comparative Physiology and Evolution of Vision in Invertebrates. Handbook of Sensory Physiology*, vol 7 / 6 / 6 A. pp. 503-580.

Molday, R. S. & Moritz, O. L. (2015). Photoreceptors at a glance. *Journal of Cell Science*, 128(22), pp 4039–4045.

Moreno-García, A., Kun, A., Calero, O., Medina, M. & Calero, M. (2018). An overview of the role of lipofuscin in age-related neurodegeneration. *Frontiers in Neuroscience*, vol. 12, pp. 464–464.

Mowat, F. M., Petersen-Jones, S. M., Williamson, H., Williams, D. L., Luthert, P. J., Ali, R. R. & Bainbridge, J. W. (2008). Topographical characterization of cone photoreceptors and the area centralis of the canine retina. *Molecular Vision*, 14, pp 2518–2527.

Neumeyer, C. (1985). An ultraviolet receptor as a fourth receptor type in goldfish color vision. *Naturwissenschaften*, 72, pp 162–163.

Ofri, R. (2013). Optics and physiology of vision. I: Gelatt, K.N., Gilger, B.C. & Kern, T.J. (eds.), *Veterinary Ophthalmology*. 5th Ed. Ames, Iowa: Wiley-Blackwell, pp. 208-270.

Pepperberg, D. R. & Masland, R. H. (1978). Retinal-induced sensitization of light-adapted rabbit photoreceptors. *Brain Research*, 151(1), pp 194–200.

Prince, M. J. *World Alzheimer Report 2015: The Global Impact of Dementia*. [online] (2015-08-25). Available from: https://www.alz.co.uk/research/world-report-2015. [Accessed 2018-12-17].

Reichenbach, A. & Robinson, S. R. (1995). The involvement of Müller cells in the outer retina. In: Djamgoz, M. B. A., Archer, S. N., & Vallerga, S. (eds.) *Neurobiology and Clinical Aspects of the Outer Retina*. pp 395–416. Dordrecht: Springer Netherlands. ISBN 978-94-011-0533-0.

Rosolen, S. G., Rigaudière, F., LeGargasson, J.-F., Chalier, C., Rufiange, M., Racine, J., Joly, S. & Lachapelle, P. (2004). Comparing the photopic ERG i-wave in different species. *Veterinary Ophthalmology*, 7(3), pp 189–192.

Sarna, T. (1992). Properties and function of the ocular melanin--a photobiophysical view. *Journal of Photochemistry and Photobiology. B, Biology*, 12(3), pp 215–258.

Schnitzer, J. (1988). Chapter 7: Astrocytes in mammalian retina. *Progress in Retinal Research*, 7, pp 209–231.

Strauß, O. (2014). Transport mechanisms of the retinal pigment epithelium to maintain of visual function. *Heat and Mass Transfer*, 50(3), pp 303–313.

Tan, K. E. (1975). Factors in the yellowing process of the human eye lens. *Ophthalmologica. Journal International D'ophtalmologie. International Journal of Ophthalmology. Zeitschrift Fur Augenheilkunde*, 171(4–5), pp 247–248.

Theuerkauf, J., Jędrzejewski, W., Schmidt, K., Okarma, H., Ruczyński, I., Śniezko, S. & Gula, R. (2003). Daily patterns and duration of wolf activity in the Białowieza Forest, Poland. *Journal of Mammalogy*, 84(1), pp 243–253.

Tovée, M. J. (1995). Ultra-violet photoreceptors in the animal kingdom: their distribution and function. *Trends in Ecology & Evolution*, 10(11), pp 455–460.

Turney, C., Chong, N. H. V., Alexander, R. A., Hogg, C. R., Fleming, L., Flack, D., Barnett, K. C., Bird, A. C., Holder, G. E. & Luthert, P. J. (2007). Pathological and electrophysiological features of a canine cone–rod dystrophy in the Miniature Longhaired Dachshund. *Investigative Ophthalmology & Visual Science*, 48(9), pp 4240–4249.

Vaney, D. I., Sivyer, B. & Taylor, W. R. (2012). Direction selectivity in the retina: symmetry and asymmetry in structure and function. *Nature Reviews Neuroscience*, 13(3), pp 194–208.

Wachtmeister, L. (1998). Oscillatory potentials in the retina: what do they reveal. *Progress in Retinal and Eye Research*, 17(4), pp 485–521.

Weleber, R.G. (1981). The effect of age on human cone and rod ganzfeld electroretinograms. *Investigative Ophthalmology & Visual Science*, vol. 20 (3), pp. 392–399.

Winter, Y., López, J. & von Helversen, O. (2003). Ultraviolet vision in a bat. *Nature*, 425(6958), pp 612–614.

Yokoyama, S. (2000). Molecular evolution of vertebrate visual pigments. *Progress in Retinal and Eye Research*, 19(4), pp 385–419.

Yokoyama, S. & Radlwimmer, F. B. (2001). The molecular genetics and evolution of red and green color vision in vertebrates. *Genetics*, 158(4), pp 1697–1710.

Zrenner, E. & Gouras, P. (1979). Blue-sensitive cones of the cat produce a rodlike electroretinogram. *Investigative Ophthalmology & Visual Science*, 18(10), pp 1076–1081.